Numerical integrators in dynamical astronomy: an overview

Iharka Szücs-Csillik

Astronomical Institute of Romanian Academy
Astronomical Observatory Cluj-Napoca
E-mail: iharka@gmail.com

March 29, 2023

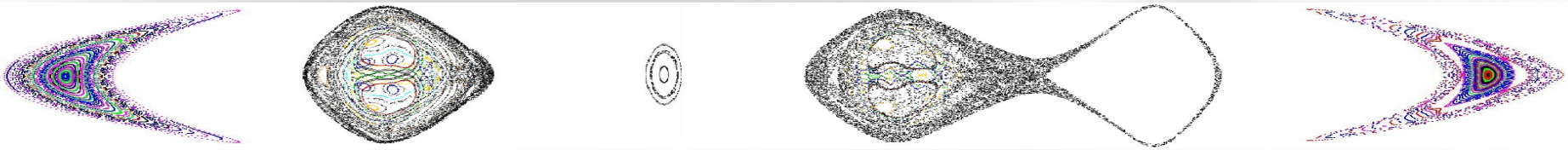

Instead of an Abstract

A Philosopher Lecturing On The Orrery By Joseph Wright Of Derby 1776 (Mechanical Model Solar System)

Content

- Decision-forecast
- Historical prediction - Chaos
- Remove the singularity
- Collision, Capture, Close encounters
- Some Regularization
- Solar system
- A little theory
- Generating function - canonical integration
- Few symplectic integrators
- Recent studies
- Near Future
- Conclusion

Decision-making

In many areas, decision-making is affected by the difficulty in producing reliable forecasts. The behavior of financial markets, consumers or weather phenomena, the evolution of an ecosystem or the movement of certain celestial bodies provide some examples of unpredictable events that have an impact on human activity.

Prediction

Some developments of mathematics can help reduce this unpredictability or, at the very least, analyze it from a strategic point of view. The theory of probability plays such a role but so do fluid mechanics in the study of turbulence, or dynamic systems in the study of so-called chaotic phenomena, which belong to a specific class of unpredictable phenomena.

Historically, the theory of dynamic systems did not immediately provide forecasting tools.

Henri Poincaré - The royal prize

King Oscar II of Sweden and Norway (1872-1907), announced a competition for a prize of 2500 kroner together with a gold medal to celebrate his 60th birthday to anyone who could prove that the Solar system was stable and would not fly apart at some future date. Henri Poincaré (1854-1912), who was a brilliant mathematician and physicist, took on the challenge and won the prize for his paper "On the problem of three bodies and the equations of equilibrium". The prize competition was announced in Acta Mathematica, written by the Swedish mathematician Gösta Mittag-Leffler.

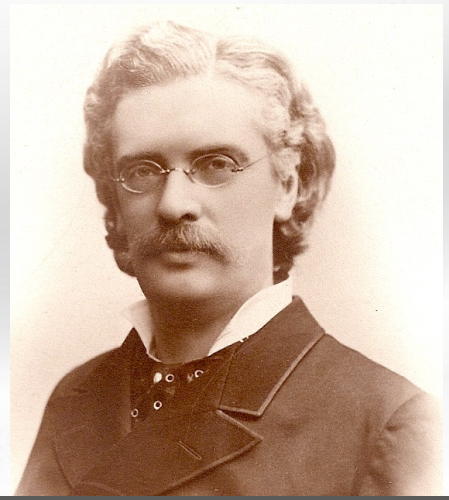

Henri Poincaré - The unpredictable

When Mittag-Leffler made his final presentation to the king on 20 January 1889, only the brief summary from Weierstrass was enclosed in the general report.
In July 1889, Mittag-Leffler decided that it was time to take action and print Poincaré's dissertation. He was a little concerned by a technical objection that had been raised. Poincaré thought the objection could easily be overcome, but as he delved deeper, he had a sudden attack of panic... He recognised chaos as an almost impossible topic to analyse mathematically. But how?


H. POINCARÉ.
»EN AF ALLA TIDERS FRÄMSTE MATEMATIKER».

H. 8 Dn STOCKHOLMSFOTOGRAF. Klichéer: Bengt Silfversparre.
Professor Poincaré (1) med sin värd, professor Mittag-Leffler (2) å Djursholm.

Poincaré - From stability...

On the last day of November 1889, a telegram reached Mittag-Leffler. Poincaré briefly told him to stop the presses. He had found an error: "It is not true that the asymptotic surfaces are closed". Trajectories near a saddle point did not converge. His proof of stability was wrong!

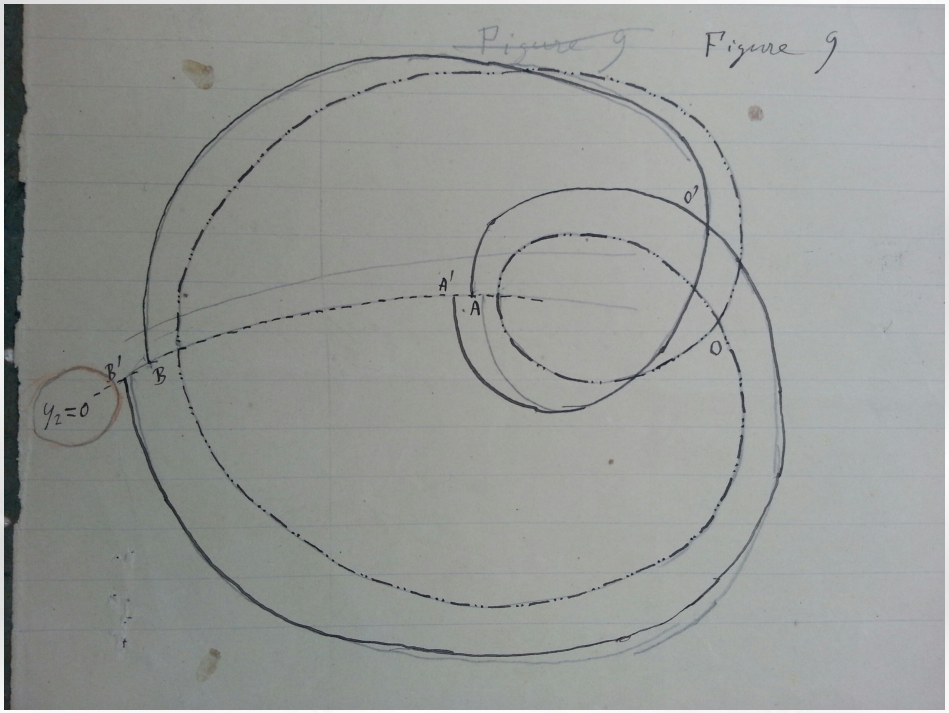

Poincaré - ...to chaos

Mittag-Leffler decided to keep his confidence in Poincaré and let him work out a revised version. He was assiduous in trying to get all the distributed copies back, without revealing any details. Poincaré was asked to pay for the first printing, which he accepted. The expenses amounted to over 3500 kroner. After intense work in December, and over Christmas and New Year, Poincaré was ready to submit a substantially revised memoir on 5 January 1890. Instead of stability for the restricted three-body problem, he had come to the inevitable conclusion that chaotic motion could occur.

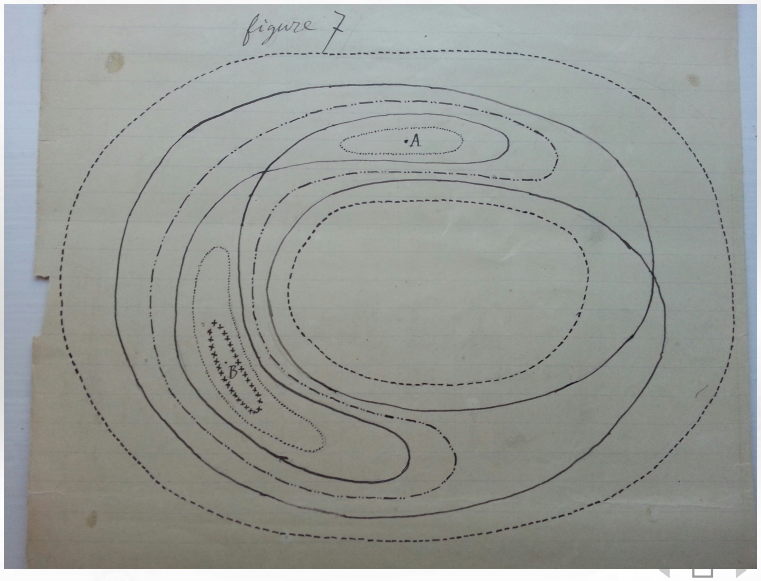

Henri Poincaré's conclusions

Poincaré (1890) proved that unlike the two-body problem that is integrable and thus its solutions are completely understood, the three-body problem is not integrable. The trajectories of the bodies depend on their masses, coordinates and velocities at the beginning. In reality, the motion can look very different if the initial conditions are modified, even by minor changes. In most cases, trajectories of the three-body system are chaotic (i.e. non-periodic), unpredictable. In some special cases, there indeed exist periodic orbits. Poincare indicates that we must use numerical algorithms to solve this problem.

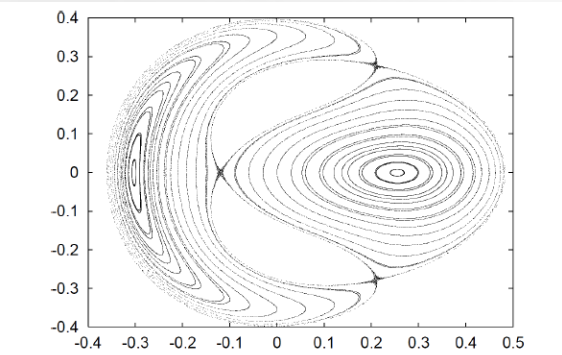

Fig. 1 – Poincaré section of the Hénon-Heiles equation (49) using RK4 integrator.

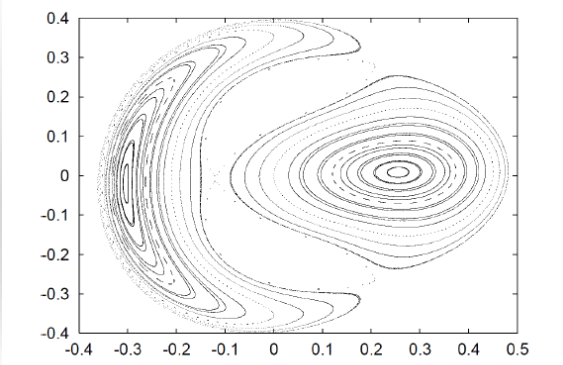

Fig. 2 – Poincaré section of the Hénon-Heiles equation (49) using SI4 integrator.

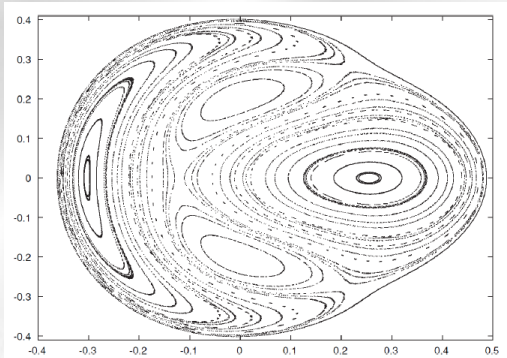

Fig. 3 – Poincaré section of the Hénon-Heiles equation (49) using LIE4 integrator.

Historical conclusions

- Lorenz (2006) found that computer-generated trajectories of chaotic systems are also sensitive to algorithms:

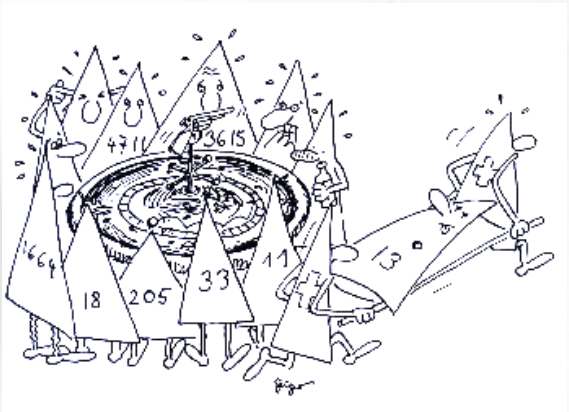

different numerical algorithms might give distinctly different computer-generated trajectories of chaotic systems after a long time.

- Consequently, we look to perform numerical simulations to describe the motion. This is made by numerical integrations in which the accuracy of the computer and the calculations are essential.
- The goal is to utilize an adequate method for obtaining precise solutions over a long time.

Problem with numerical calculations

- needs sophisticated algorithms to avoid build up errors;
- difficult to parallelize;
- typical calculations last several months;
- roundoff errors!

Finance - new Vancouver stock exchange index was initialized in 1982 at 1000. After 22 months the index stood at 524.881 despite a rising market. Gulf War (1991) - Patriot missile defense system converted clock steps of 0.1s to decimal by multiplying by a 22-bit binary number. After 100 hours the accumulated roundoff error was 0.3s, which led to failure to intercept a Scud missile, resulting in 28 deaths. Hence, always use highest possible precision.

Problem at collsion

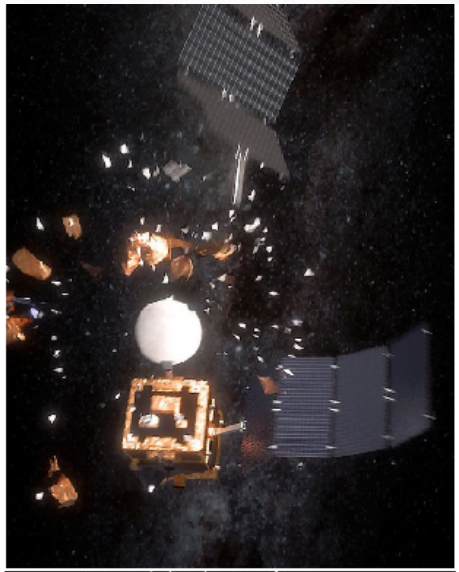

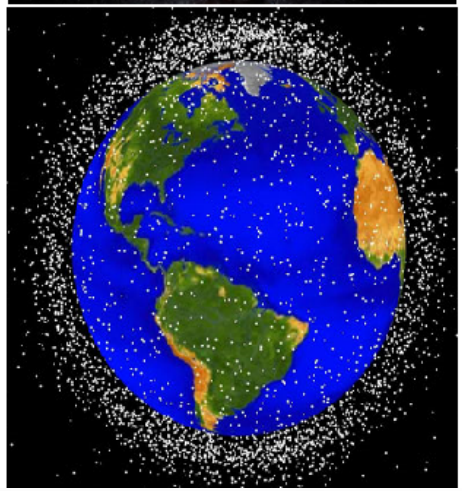

What is happening at close encounters?

- At the collision, the equations of motion show singularities. When the distance between the bodies approaches zero (close encounters), then the forces acting between particles approach infinity, and this event produces sharp bends of the orbit. The numerical precision after the collision will be worse because of the round-off and truncation errors.
- At close encounters, where not actually singularities occur, we can use time-step control decreasing the size of the time-steps. The numerous small-time steps will introduce numerical errors. In contrast, all solutions can be determined analytically or numerically if the singularities are eliminated (regularization method).
- The removal of the singularity from the Hamiltonian does not necessarily imply the absence of singular terms in the equations of motion. The continuation of the orbit after close encounters (collision) is not feasible since the solution encounters the singularity present in the problem.

Close approach of comet Oterma

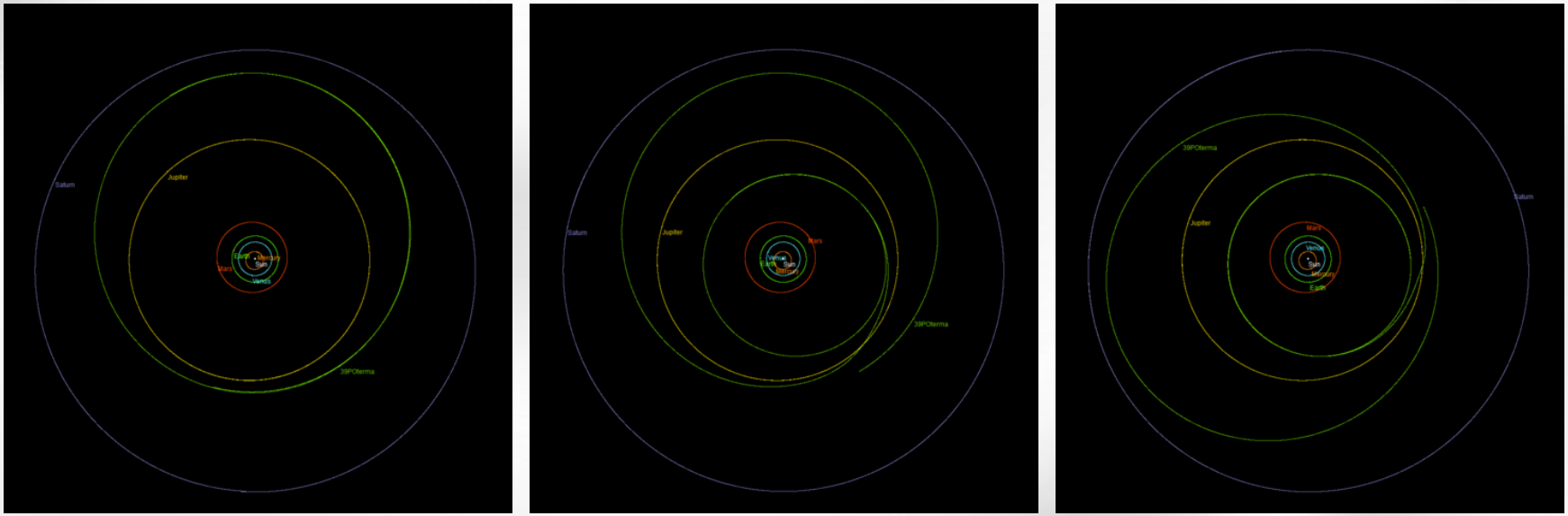

Orbit of Saturn, Comet 39P/Oterma, Jupiter. a. Before 1930; b. 1920-1950; 1945-1983

39P/Oterma close approaches to planets

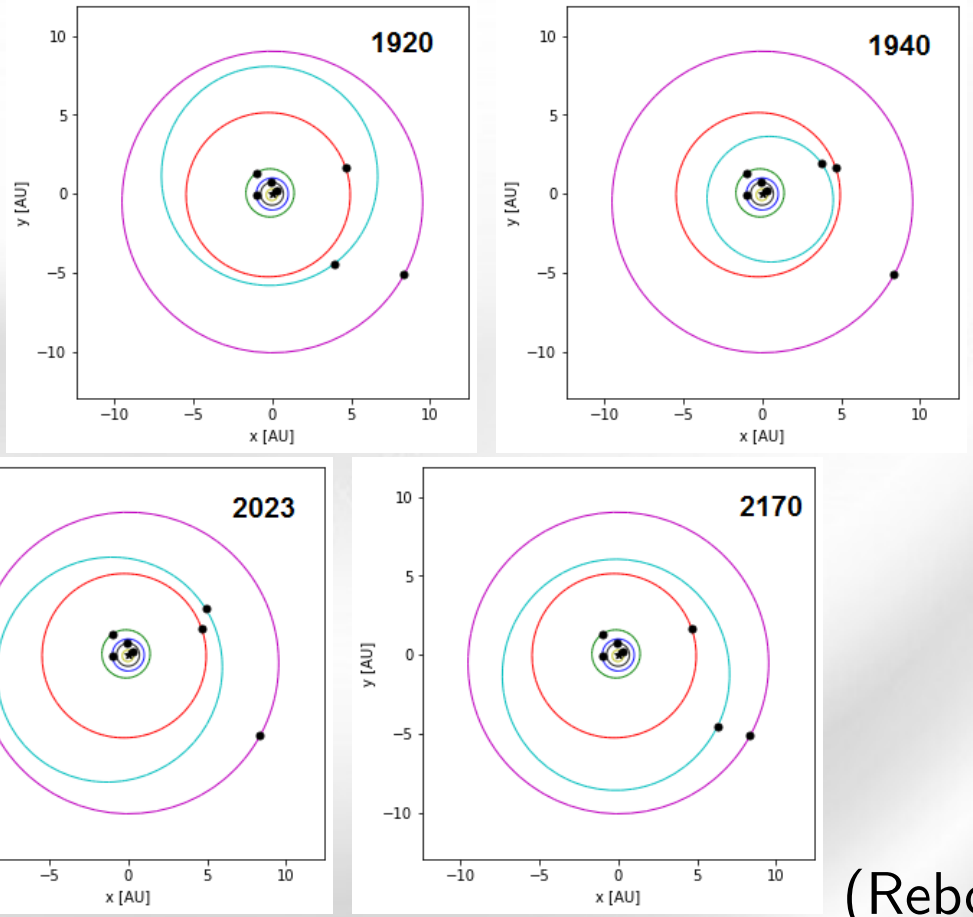

(Rebound)

1963-Apr-12 Jupiter 0.095 AU 2011-Jun-03 Saturn 1.014 AU

2025-Jan-15 Jupiter 0.888 2155-Feb-21 Jupiter 0.771

2168-Oct-03 Saturn 1.933 (NASA Horizon)

About the capture of comet Oterma

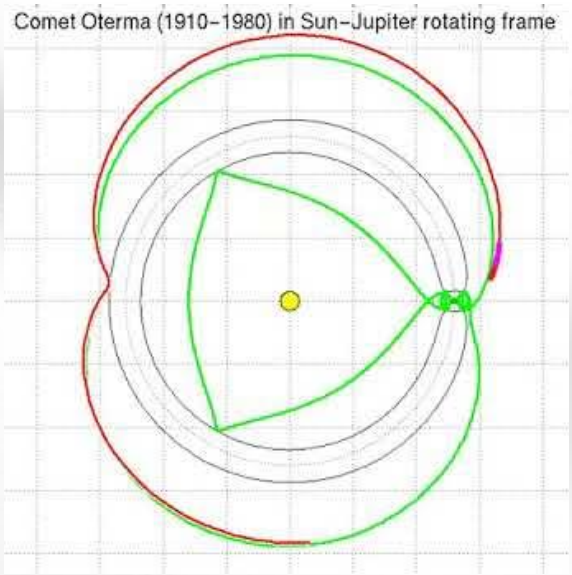

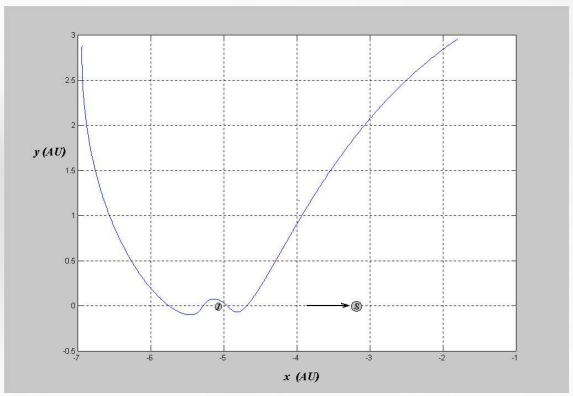

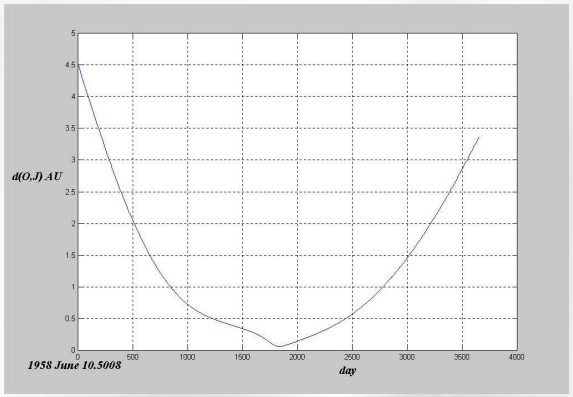

a. Capture of Comet 39P/Oterma; b. Close distance between 1958-1968; Close approach between 1958-1968.

See: Koon, W.S., M.W. Lo, J.E. Marsden and S.D. Ross: Resonance and capture of Jupiter comets, Celestial Mechanics and Dynamical Astronomy 81(1-2), p. 27-38, 2001.

Szenkovits, F., Makó, Z., Csillik, I., Bálint, A.: Capture model in the restricted three body problem. Pure Mathematics and applications 13(4), p. 463-471, 2002.

Resonant capture

- Why is Oterma not colliding with Jupiter? Resonance transition - interior-exterior resonances - outside 2:3, inside 3:2. (See Theory of Tube Dynamics, lobe dynamics, transport theory for minor bodies.)
- Why don't Pluto and Neptune collide? Resonance 3:2 ensures that Pluto only crosses Neptun's orbit, when it is 90 degrees away from Neptune.
  - Early in the Solar system there was planetesimals (debris) between planets. Ejection of this debris by Neptune caused its orbit to migrate outwards.
  - If Pluto were initially in a circular orbit outside Neptune, it was captured into 3:2 resonances, and its eccentricity and inclination grow as Neptune continues to migrate outwards.

Remove the singularity

- The numerical difficulties associated with integrations of close two-body encounters can be avoided by introducing regularizing transformations which remove the singularity.

- In 1765, Euler proposed regularizing transformations when studying the rectilinear motion.
- Regularization is defined as the elimination of singularities occurring in the equations of motion by properly selected variables.

LC - Kepler problem vs. Harmonic oscillator


```
Kepler problem:
function pr=pr2(t,y);
    r=sqrt(y(1)^2+y(3)^2);
    pr(1)=y(2);
    pr(2)=-y(1)/r^3;
    pr(3)=y(4);
    pr(4)=-y(3)/r^3;
    pr=pr';
function output=pro2;
y0=[1 0 0 0.7];
tspan=[0 20*pi];
[t,y]=ode45('pr2',tspan,y0);
plot(y(:,1),y(:,3));
```

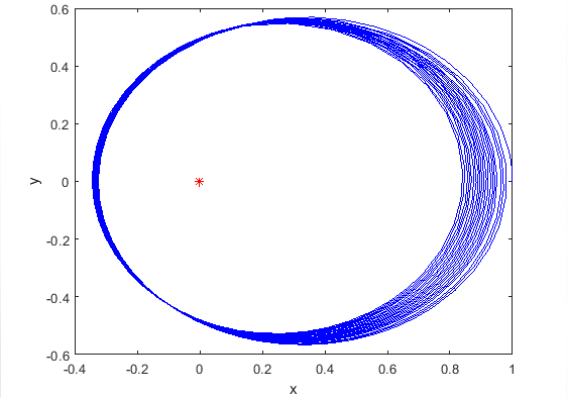

Under Levi-Civita's transformation of coordinates and time ($x = u^2 - v^2$, $y = 2uv$, $dt/ds = \sqrt{x^2 + y^2}$), a Kepler problem in (x, y) changes into a harmonic oscillator in (u, v).

```
Harmonic oscillator:
function dy=reg2(t,y);
    r2=(y(1)^2+y(3)^2);
    v2=(y(2)^2+y(4)^2);
    C=(8-v2)/(4*r2);
    dy(1)=y(2);
    dy(2)=-4*C*y(1);
    dy(3)=y(4);
    dy(4)=-4*C*y(3);
    dy=dy';
function output=reg2;
y0=[1 0 0 0.35];
tspan=[0 39.6434];
[t,y]=ode45('reg2',tspan,y0);
plot(y(:,1),y(:,3));
```

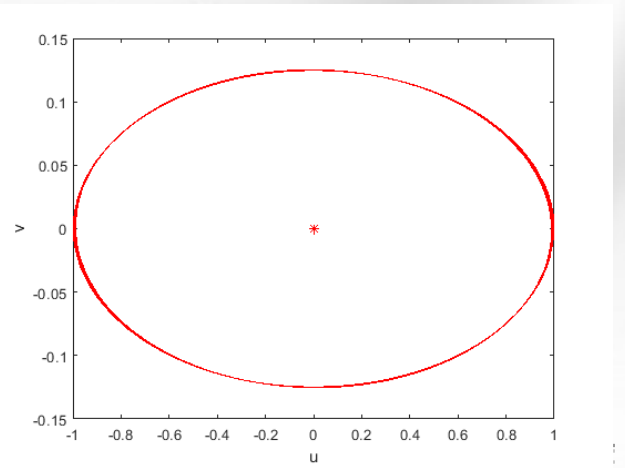

Configuration space vs phase space

Lagrangian dynamics

Points in the n-**dim configuration space** correspond to given configu rations. The coordinates of a point are the n generalized coordinates q_k of a dynamical system $k = \overline{1, n}$.

$q_k = q_k(t, q_k^0, \dot{q}_k^0)$

Hamiltonian dynamics

Points in the $2n$-**dim phase space** correspond to definite state of the system. The coordinates of a point are the n generalized coordinates q_k and the n generalized momenta p_k of a dynamical system $k = \overline{1, n}$.

(q_k, p_k)

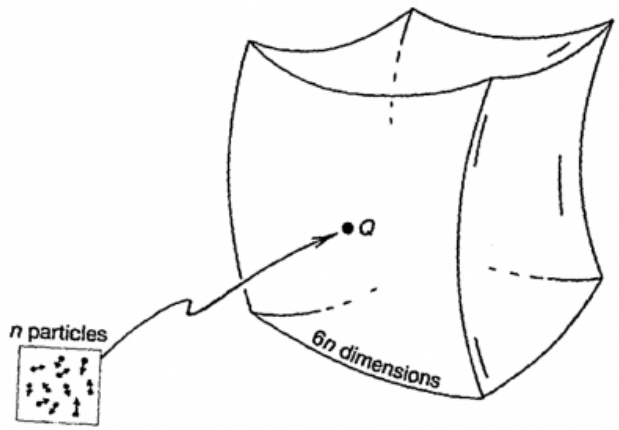

Fig. 5.10. Phase space. A single point Q of phase space represents the entire state of some physical system, including the instantaneous motions of all of its parts.

LC - Double angles at the origin R3BP

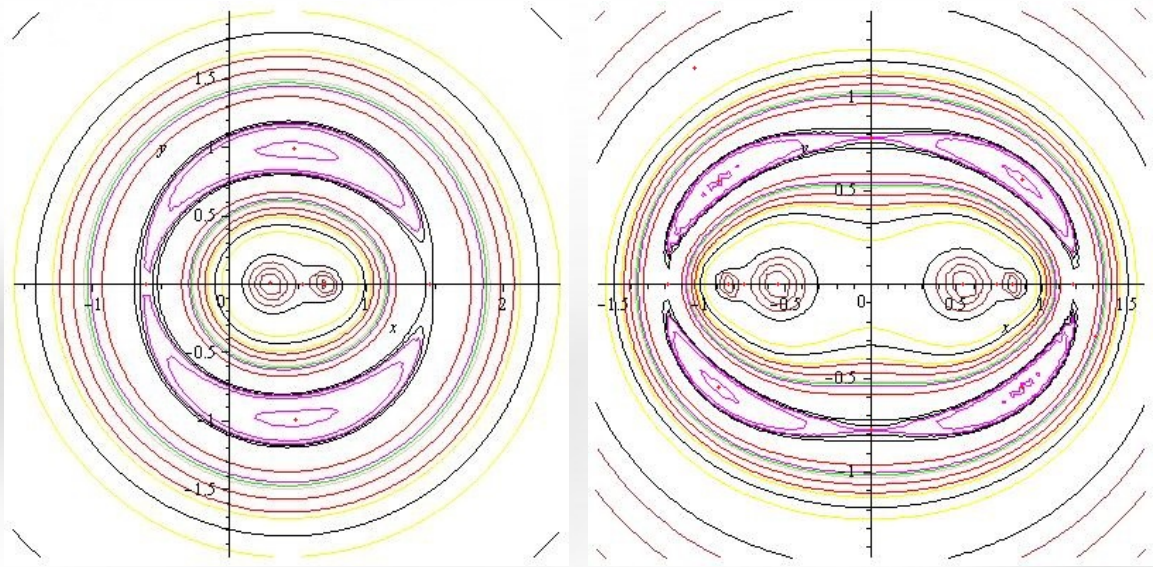

Hill's region configurations for the CR3BP system when $\mu = 0.3$. The lines depict the Zero Velocity Curves (ZVCs) in the CR3BP and in the LC-regularized CR3BP. The contours denote values of the Jacobi integral. The surface also only predicts what regions can not be entered, not the shape of the trajectory within the surface. 3.05-3.09 - small forbidden region around L4 and L5 start to grow, 3.1 - the neck around L1 and L3 are open, 3-4 - the neck around L1 is open, 4-10 decrease the ZVC around the two center, 10-21 - No transit orbits among the three regions are possible.

McGehee - Local regularization in R3BP

Levi-Civita method remove the singularity by introducing the parametric u-plane using the simplest mapping of the u plane onto the x-plane satisfying the requirement to double angles at the origin an be conformal elsewhere.

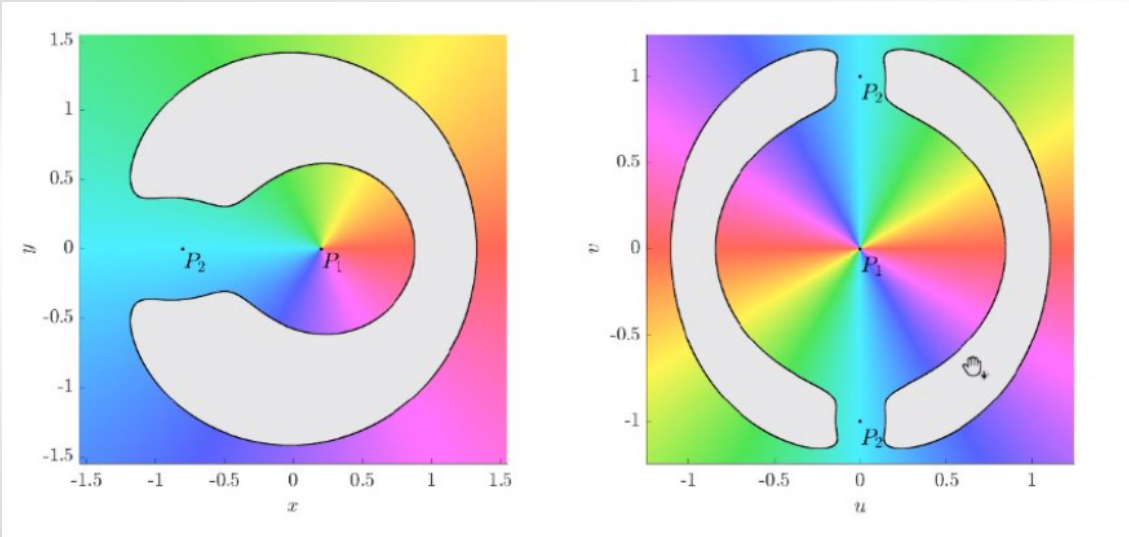

Mercé Ollé, Oscar Rodriguez, Jaume Soler: Local regularization in the R3BP and ejection-collision orbits.

McGehee's regularization R3BP

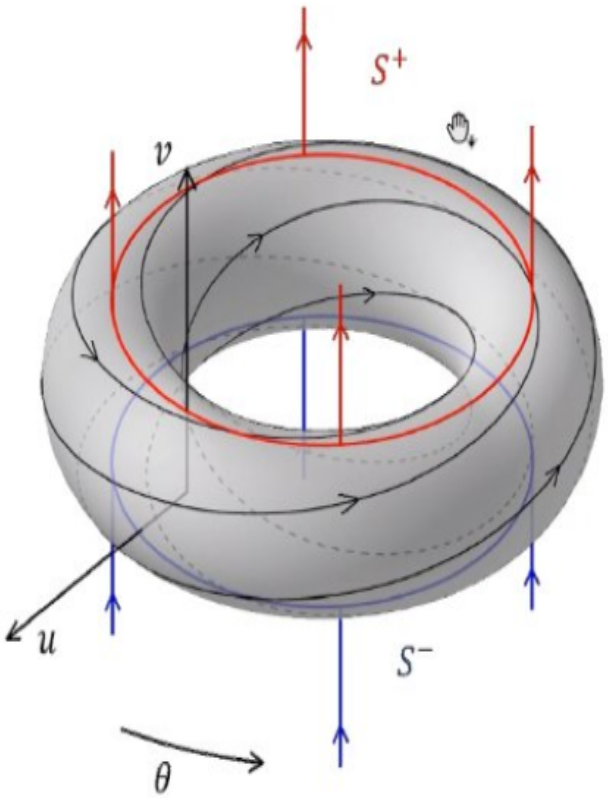

- $W^u(S^+)$: Set of ejection orbits.
- $W^s(S^-)$: Set of collision orbits.

EC orbits

Set of orbits obtained from the intersection $W^u(S^+) \cap W^s(S^-)$.

An EC orbits is an heteroclinic connection between $p \in S^+$ and $q \in S^-$.

McGehee's regularization 2BP

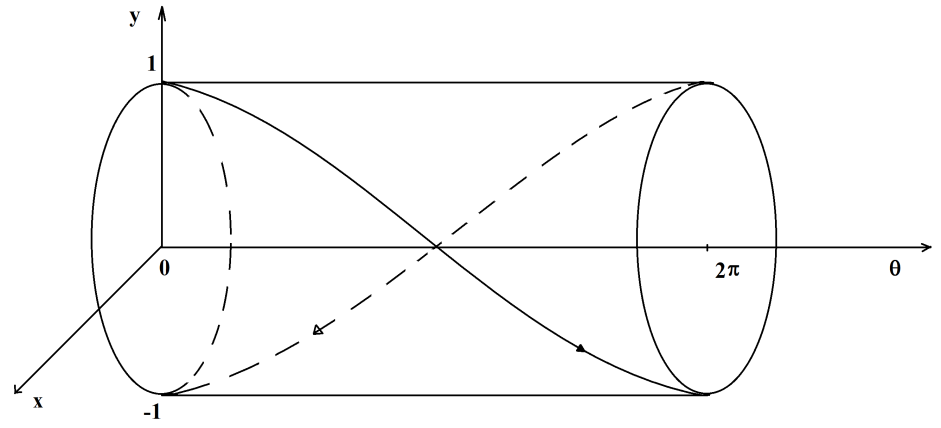

$$
\begin{aligned}
r &= |\mathbf{q}| \\
\theta &= atan\frac{q_2}{q_1} \\
u &= \dot{r} = \frac{q_1 p_1 + q_2 p_2}{|\mathbf{q}|} \\
v &= r\dot{\theta} = \frac{q_1 p_2 - q_2 p_1}{|\mathbf{q}|}
\end{aligned}
$$

$$
\begin{aligned}
x &= u\sqrt{r} \\
y &= v\sqrt{r} \\
\frac{dt}{ds} &= r^{3/2}
\end{aligned}
$$

$$
\begin{aligned}
r' &= rx \\
\theta' &= y \\
x' &= x^2/2 + y^2 - 1 \\
y' &= -xy/2
\end{aligned}
$$

$$M_{col} = \{(r, \theta, x, y)/r = 0, \theta \in \mathbb{S}^1, x^2 + y^2 = 2\}$$

KS - regularization in 3D

As we know, the differential equations of motion of relative two-body problem $\ddot{\mathbf{r}} = -\frac{\mu \mathbf{r}}{r^3}$ are singular at $r = 0$. Therefore, in a fixed reference frame, in space, with relative Cartesian coordinates $\mathbf{q} = (q_1, q_2, q_3)$, the two-body problem is described by the Hamiltonian as

$$H(q_i, p_i) = \frac{\sum_{i=1}^{3} p_i^2}{2} - \frac{\mu}{\sqrt{\sum_{i=1}^{3} q_i^2}}, \tag{1}$$

with the corresponding canonical equations:

$$\begin{aligned} \dot{q}_i &= p_i, \\ \dot{p}_i &= -\frac{\mu q_i}{(q_1^2 + q_2^2 + q_3^2)^{3/2}} = -\frac{\mu q_i}{r^3}, \end{aligned} \tag{2}$$

where q_i and p_i, $i = \overline{1,3}$ are the canonical coordinates in physical space.

KS - transformations

In order to achieve the regularization in space, we introduce the $L(\mathbf{Q})$ - KS-matrix, which is orthogonal $L^T(\mathbf{Q})L(\mathbf{Q}) = rE$, where E is the identity matrix, and L^T is the transpose of L matrix, $\mathbf{Q}$ is the new coordinates in parametric space:

$$L(\mathbf{Q}) = \begin{pmatrix} Q_1 & -Q_2 & -Q_3 & Q_4 \\ Q_2 & Q_1 & -Q_4 & -Q_3 \\ Q_3 & Q_4 & Q_1 & Q_2 \\ Q_4 & -Q_3 & Q_2 & -Q_1 \end{pmatrix} \tag{3}$$

As a first step, we introduce the KS transformation, which transforms the $(q_1, q_2, q_3, p_1, p_2, p_3)$ coordinates and momenta in 3-dimensional physical space into the $(Q_1, Q_2, Q_3, Q_4, P_1, P_2, P_3, P_4)$ new coordinates and momenta in 4-dimensional parametric space:

$$\mathbf{q} = \mathbf{L}(\mathbf{Q}) \cdot \mathbf{Q}, \tag{4}$$

where $q_4 = 0 = Q_4 Q_1 - Q_3 Q_2 - Q_2 Q_3 + Q_1 Q_4$ is the bilinear relation.

KS - regular equations

The new Hamiltonian derived from the *KS* transformations is:

$$\overline{H}_{KS} = \frac{1}{8} \cdot \frac{\sum_{i=1}^{4} P_i^2}{r} - \frac{\mu}{r}, \qquad r = \sum_{i=1}^{4} Q_i^2. \tag{5}$$

In the second step, we adopt the new fictitious time s as a time transformation:

$$\frac{dt}{ds} = r. \tag{6}$$

Consequently, the new canonical, regular equations become:

$$\begin{aligned} \frac{dQ_i}{ds} &= P_i/4\ , \\ \frac{dP_i}{ds} &= 2\overline{H}_{KS_2} Q_i, \quad i = \overline{1,4}\ , \end{aligned} \tag{7}$$

where the energy $\overline{H}_{KS}$ is constant.

Why to apply KS regularization?

- Increasing the order of the new canonical equations of motion (7) is not a disadvantage from the numerical point of view, because the regularized equation are more efficient. The KS transformation regularizes the corresponding equations of motion allowing us to understand the near-collision dynamics.
- The KS transformation blows up the motion's area near the singularity, and slows down the motion in the parametric plane, using the fictitious time.
- The *KS* regularization is a simple regularization model for the study of motion in physical space. It can be used as a first approximation in regularizing studies.
- Using the generalization of the KS-coordinate transformations one can study the orbit's shape of a given celestial object even with small eccentricity around the singularities.

Solar system

- Copernicus (1543), Kepler (1619)
- Newton (1687), Euler (1765)
- Poincaré (1890), Lorenz (2006)

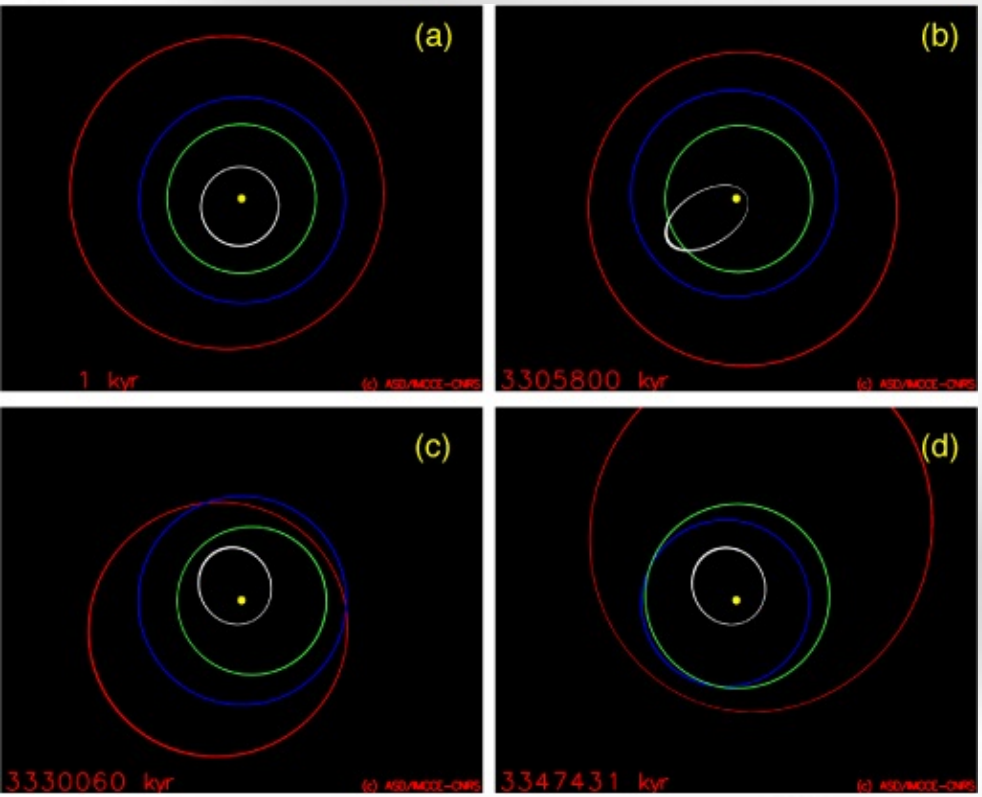

- Collision-singularities-regularization
- The question of the stability of the Solar System is one of the oldest problems in physics.
- A collision with another planet or the Sun is possible in less than 5 billion years (Gyr), before the end of the life of the Sun when it becomes a red giant.
- Mercury's orbit is unstable as found out in earlier studies.
  Mercury will be expelled (30 Myr).
  (Laskar, Gastineau, 2009;
  Mikkola, Lehto, 2022).

Batygin-Brown (2016) Evidence for a distant giant planet in the Solar system (200 AU).

Precise solution over a long time

- We look to perform numerical simulations to describe the motion. This is made by numerical integrations in which the accuracy of the computer and the calculations are essential.
- The goal is to utilize an adequate method for obtaining precise solutions over a long time.
- For long-term integrations, the most commonly used are symplectic integrators. Symplectic schemes incorporate the symmetries of Hamiltonian systems, and as a result, usually conserve the energy and angular momentum better than nonsymplectic integrators. In particular, the angular momentum is usually conserved up to a roundoff error in symplectic integrators.

Known Definitions: SI and Hamiltonian

In mathematics, a symplectic integrator (SI) is a numerical integration scheme for Hamiltonian systems.
Formally, a Hamiltonian system is a dynamical system characterised by the scalar function $H(\boldsymbol{q}, \boldsymbol{p}, t)$, also known as the Hamiltonian.
The state of the system, $\boldsymbol{r}$, is described by the generalized coordinates $\boldsymbol{p}$ and $\boldsymbol{q}$, corresponding to generalized momentum and position respectively. Both are real-valued vectors with the same dimension N. Thus, the state is completely described by the 2N-dimensional vector $\boldsymbol{r} = (\boldsymbol{q}, \boldsymbol{p})$ and the evolution equations are given by Hamilton's equations:

$$\frac{d\boldsymbol{p}}{dt} = -\frac{\partial H}{\partial \boldsymbol{q}},$$
$$\frac{d\boldsymbol{q}}{dt} = +\frac{\partial H}{\partial \boldsymbol{p}}.$$

The trajectory $\boldsymbol{r}(t)$ is the solution of the initial value problem defined by Hamilton's equations and the initial condition $\boldsymbol{r}(t = 0) = \boldsymbol{r}_0 \in \mathbb{R}^{2N}$.

Known Properties of SIs

- The Hamiltonian dynamical system has a symplectic structure, which consequence is that an infinitesimal phase space volume is preserved. A corollary of this is the Liouville's theorem: on a Hamiltonian system, the phase-space volume of a closed surface is preserved under time evolution.
- Symplectic integrator form the subclass of geometric integrator, which is a numerical method that preserves geometric properties of the exact flow of a differential equation.
- Many of these geometric properties are of crucial importance in physical applications: preservation of energy, momentum, angular momentum, phase space volume, symmetries, time-reversal symmetry, symplectic structure and dissipation are examples.
- Geometric integrators are canonical transformations. They are widely used in nonlinear dynamics, molecular dynamics, discrete element methods, accelerator physics, plasma physics, quantum physics, and celestial mechanics.

Canonical integration technique - 1

Symplectic map generates phase space behavior, which is close to that of original system.
Consider a system of differential equations governed by the Hamiltonian $H = \mathbf{p}^2/2 + V(\mathbf{q}, t)$. Its solution is given by the functions $\mathbf{q}(\mathbf{q_0}, \mathbf{p_0}, t)$ and $\mathbf{p}(\mathbf{q_0}, \mathbf{p_0}, t)$.
Due to the canonical character of these equations of motion constitutes a canonical transformation (symplectic map) from initial conditions at $t = 0$ to the state vector at time t: $(q, p) = M(t)(q_0, p_0)$.
If t is small, can this map be found approximately to some given order in t?
The n-th order symplectic map is $(q, p) = M_n(t)(q_0, p_0)$, where n is the order of the map $\|M(t) - M_n(t)\| = O(t^{n+1})$.

Canonical integration technique - 2

Let (q_1, p_1) the new coordinates. The convenient form for generating function of the canonical transformation $(q, p) \rightarrow (q_1, p_1)$ is that involving new coordinates and old momenta: $F_3(q_1, p, t) = -q_1 p + G(q_1, p, t)$.

$$\begin{aligned} q &= -\frac{\partial F_3}{\partial p} = q_1 - G_p, \quad p_1 = -\frac{\partial F_3}{\partial q_1} = p - G_{q_1}, \\ H_1 &= H + \frac{\partial F_3}{\partial t} = H + G_t. \end{aligned}$$

These equations suggest to select $G = -\{p^2/2 + V_1(q_1, t)\}t$, so that

$$\begin{aligned} p_1 &= p - f(q_1, 0)t, \quad f(q, 0) = -\frac{\partial V(q, 0)}{\partial q}, \\ q &= q_1 + pt, \\ H_1 &= V(q_1 + t(p_1 + f(q_1, t), t), t) - V(q_1, 0). \end{aligned}$$

And expanding on the small parameter t:

$H_1 = tV_t(q_1, 0) - tp_1 f(q_1, 0) + O(t^2) \rightarrow$

$q_1 = const + O(t^2), \qquad p_1 = const + O(t^2).$

Leapfrog method schema

The leapfrog method is numerically integrating differential equations as the form of canonical equations of the two-body problem, namely

$$\dot{q}_i = p_i, \qquad \dot{p}_i = -\frac{\mu q_i}{(q_1^2 + q_2^2 + q_3^2)^{\frac{1}{2}}} = -\frac{\mu q_i}{\mathbf{r}},$$

where q_i and p_i, $i = \overline{1,3}$ are the canonical coordinates in physical space. The leapfrog integrator solves the second-order ordinary differential equations directly, it is reversible and it approximately conserves energy. The leapfrog schema for two-body problem explicitly with h step size can be written as:

$$q_i^j = q_i^{j-1} + hp_i^{j-1} - \frac{h^2 \cdot q_i^{j-1}}{2((q_1^{j-1})^2 + (q_2^{j-1})^2 + (q_3^{j-1})^2)^{\frac{3}{2}}}, \quad j = \overline{0, t_n}$$

$$p_i^j = p_i^{j-1} - \frac{h}{2}\left(\frac{q_i^{j-1}}{((q_1^{j-1})^2 + (q_2^{j-1})^2 + (q_3^{j-1})^2)^{\frac{3}{2}}} + \frac{q_i^j}{((q_1^j)^2 + (q_2^j)^2 + (q_3^j)^2}\right.$$

where $i = \overline{1,3}$, j is the time step, and t_n the final time.

Neri's 4th order symplectic integrator

The Neri's fourth-order symplectic integrator schema explicitly is given by:

$$\begin{aligned} q_i^k &= q_i^{k-1} + hc_k p_i^{k-1}, \\ p_i^k &= p_i^{k-1} - hd_k \frac{q_i^k}{((q_1^k)^2 + (q_2^k)^2 + (q_3^k)^2)^{\frac{3}{2}}}, \quad i = \overline{1,3}, \quad k = \overline{1,4}, \end{aligned} \tag{10}$$

where the value of the coefficient c_k, d_k, $k = \overline{1,4}$ are

$$\begin{aligned} c_1 &= c_4 = \frac{1}{2(2-2^{1/3})}, \qquad c_2 = c_3 = \frac{1-2^{1/3}}{2(2-2^{1/3})}, \\ d_1 &= d_3 = \frac{1}{2-2^{1/3}}, \qquad d_2 = \frac{-2^{1/3}}{2-2^{1/3}}, \qquad d_4 = 0. \end{aligned} \tag{11}$$

Note that the Neri symplectic integrator is suitable for an autonomous Hamiltonian system which can be split into two integrable parts of kinetic and potential energies (Separable Hamiltonian system).

Neri's 4th SI with 9 stages

The value of the coefficient c_k, d_k, $k = \overline{1,10}$ are:

$$
\begin{aligned}
d1 &= 0.0465; \quad d2 = 0.1549; \quad d3 = 0.3197; \quad d4 = -0.1929; \\
c1 &= 0.1289; \quad c2 = 0.1090; \quad c3 = -0.0138; \quad c4 = 0.1837; \\
d5 &= 0.5 - d1 - d2 - d3 - d4; \quad d6 = d5; \quad d7 = d4; \\
d8 &= d3; \quad d9 = d2; \quad d10 = d1; \quad c6 = c4; \quad c7 = c3; \\
c5 &= 1 - 2 * (c1 + c2 + c3 + c4); \quad c8 = c2; \quad c9 = c1; \quad c10 = 0.
\end{aligned}
$$

Note that schemes of order 6 or higher require more stages than compositions, and only fourth-order methods seem promising. Including additional stages more efficient methods can be obtained.

Non-separable symplectic integrators

$$H(Q,P) = (Q^2+1)(P^2+1)/2.$$

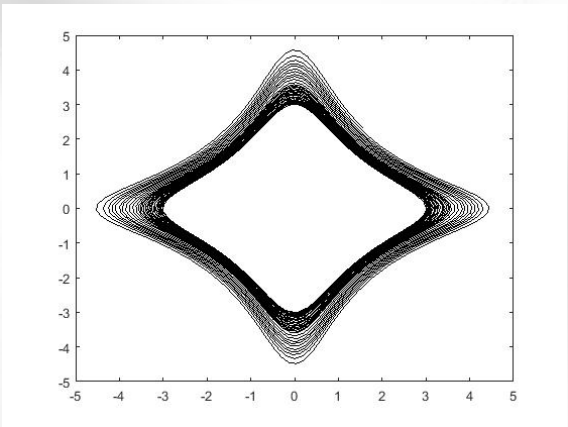
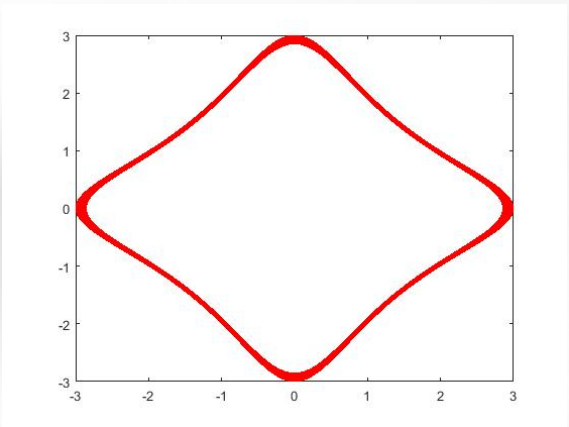
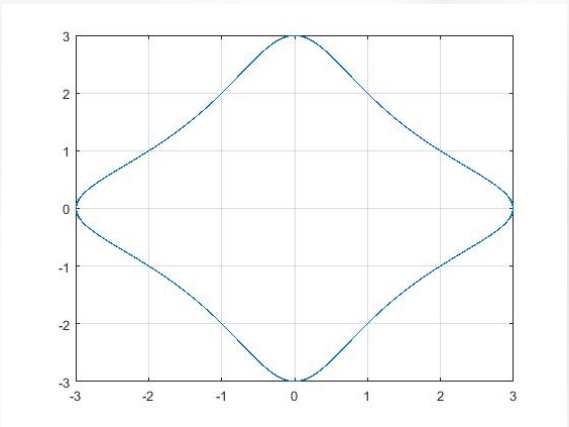

What about the non-separable Hamiltonian systems? Such as a finite-dimensional representation of the nonlinear Schrödinger equation, nearly integrable systems in action-angle coordinates for astrophysical examples, charged particle dynamics, molecular dynamics with thermostats, classical systems with post-Newtonian correction that approximates general relativity effects, etc.

Kepler problem and CR3BP

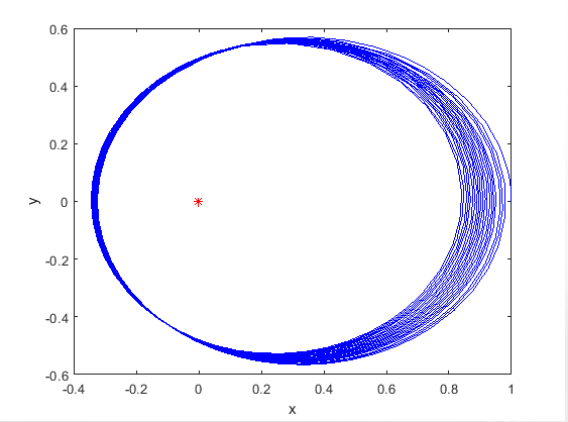

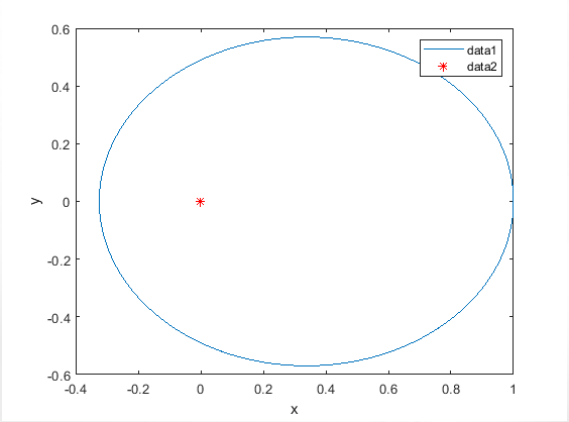

The Kepler problem using RK 4th order and Neri's 4th order symplectic integrator.

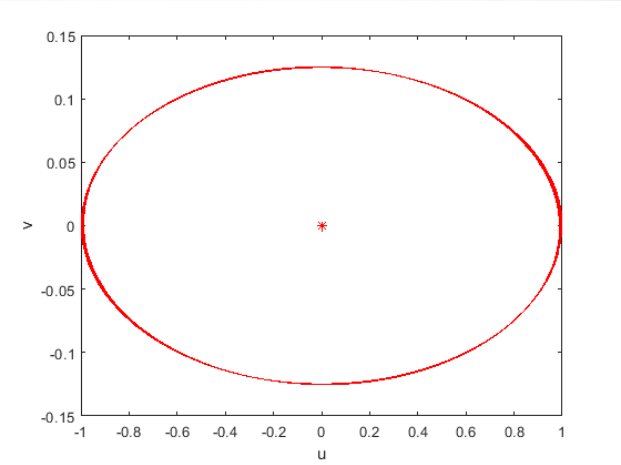

Recent studies

- Nowaday, there is an increasing need for a precise long-term integration. The first long-term direct numerical integration (without averaging) of a realistic model of the Solar System, together with the precession and obliquity equations, was performed by Quinn et al. (1991) over 3 Myr.
  The orbital motion of the full Solar System was computed over 100 Myr using a symplectic integrator with mixed variables (Wisdom and Holman, 1991).
- Following the improvement of computer technology, long-term integrations of realistic models of the Solar System have been improved (Ito and Tanikawa, 2002).
- Now it is possible to integrate the motion of the Solar System over time periods of more than 5 Gyr, which is comparable to its age or expected lifetime (Laskar and Gastineau, 2009; Laskar and Robutel, 2001; Mikkola and Lehto, 2022).

Near Future

It must be emphasized that high-performance computers and artificial intelligence (including machine learning) play significant roles in performing the investigation of the n-body problem. In the following, I will present briefly some integrators, codes, software packages that analysing also close encounter problems (see Szucs-Csillik, RoAJ 2022):

- DROMO (Peláez et al., 2007; Bau et al., 2011).
- FCIRK16 (Antonana et al., 2022).
- NBODYx (Aarseth, 2003).
- MSTAR (Rantala et al., 2020).
- FROST (Rantala et al., 2021). BIFROST (Rantala et al., 2022).
- Swifter.
- STARLAB (Anders et al., 2009).
- REBOUND (Rein and Tamayo, 2015; Rein and Spiegel, 2015).
- Orbfit (Gronchi et al., 2010).

Sample animation of many-body problem

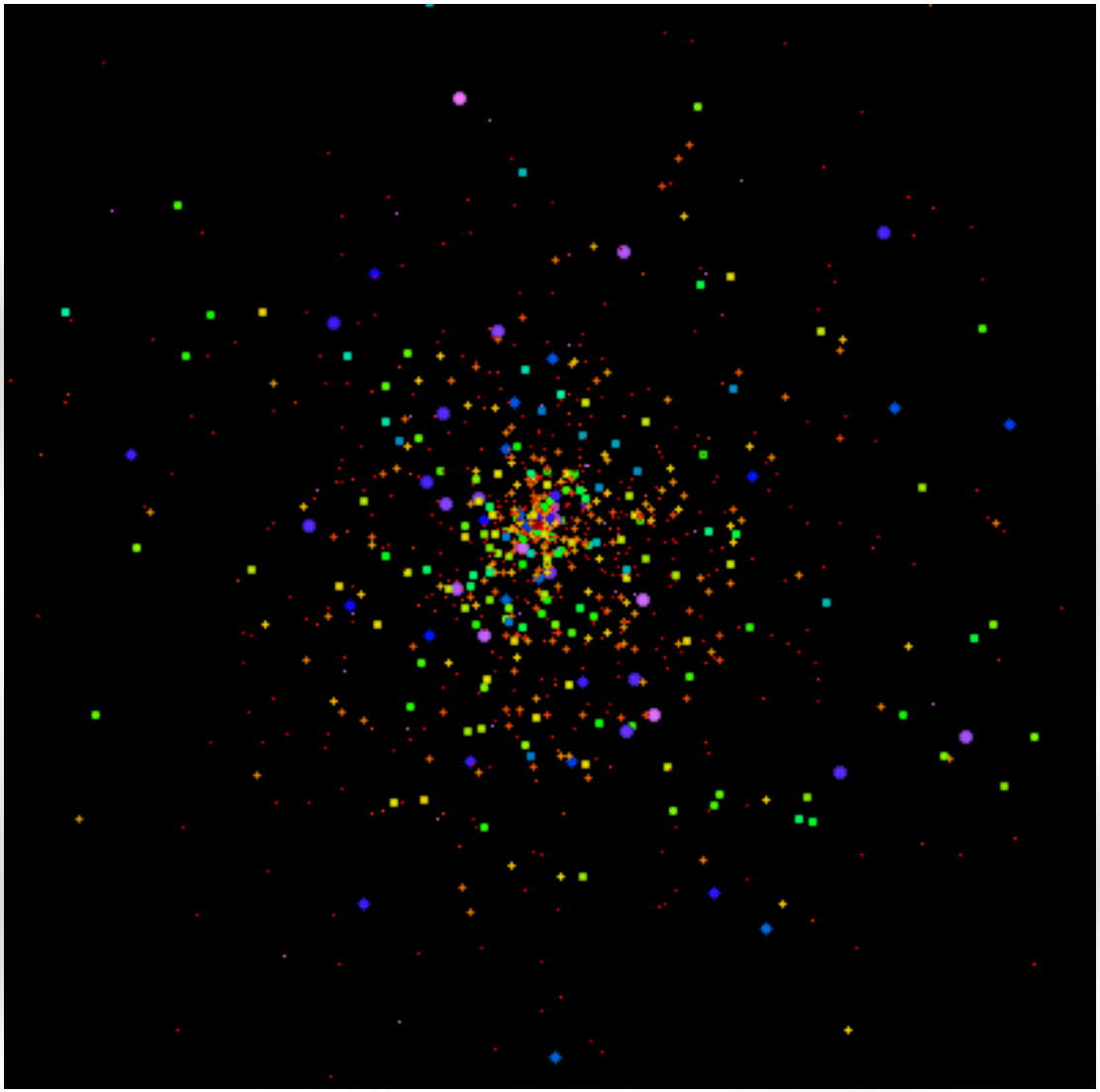

Created with the STARLAB toolset (1024 bodies).

2023 DW - Asteroid

"We've been tracking a new asteroid named 2023 DW that has a very small chance of impacting Earth in 2046," said NASA Asteroid Watch on its Twitter.

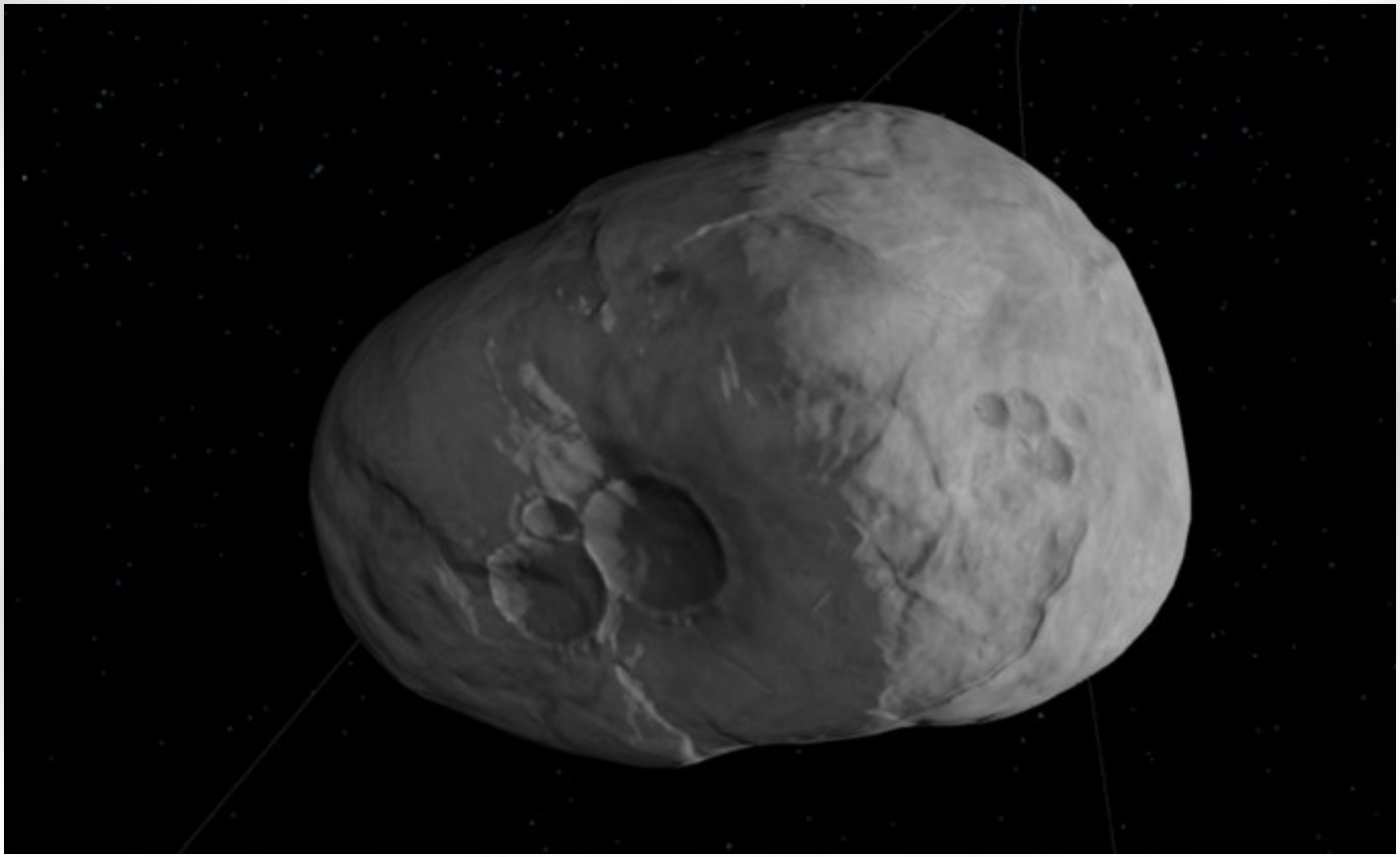

2023 DW - NASA-Jet Propulsation Laboratory

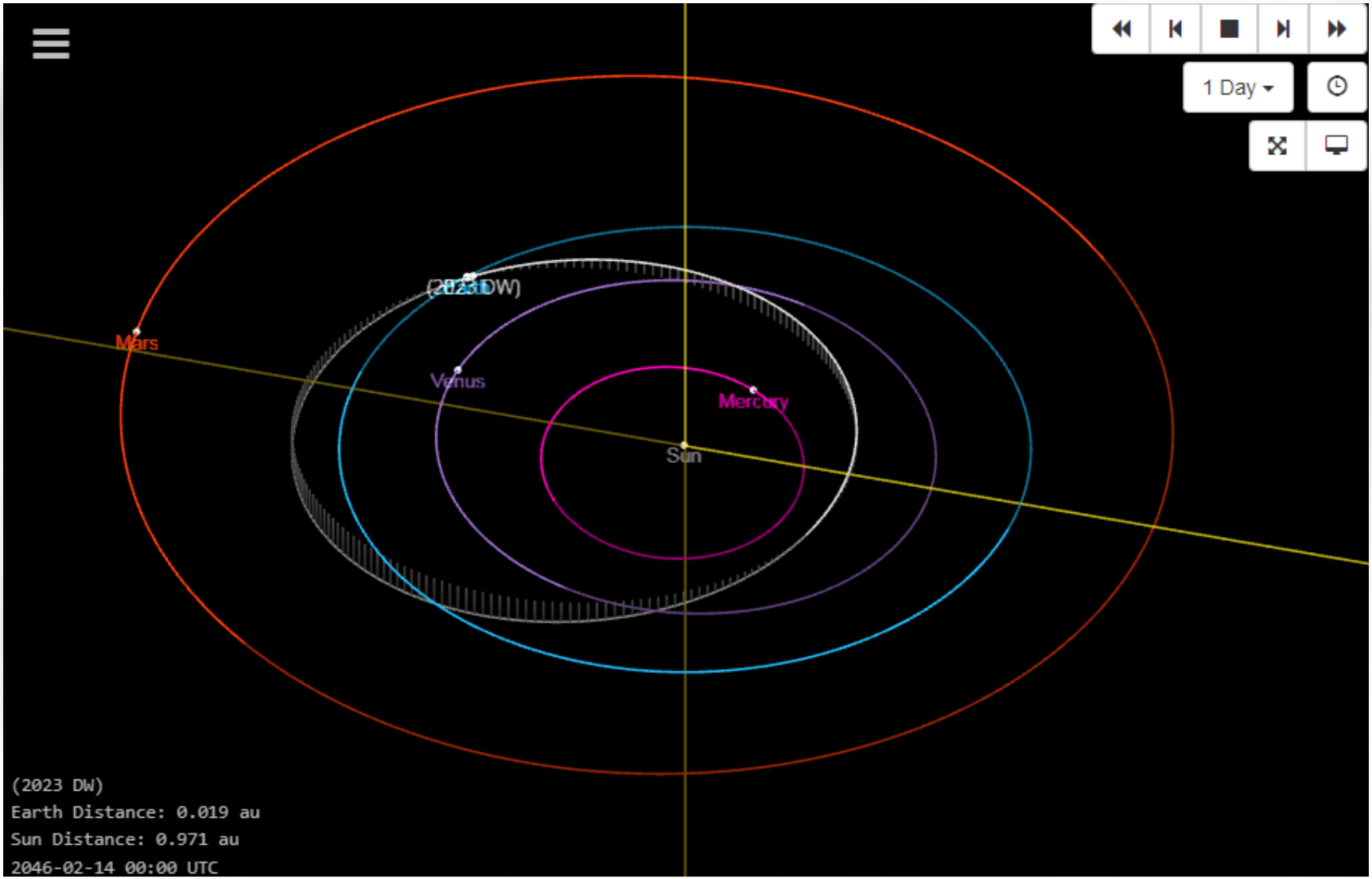

2023 DW. Neo/Aten (Orbital elements)

Discovered by Georges Attard and Alain Maury in San Pedro de Atacama at 26 February 2023.
Epoch 2023-Feb-25 (JD 2460000.5)
Semi-major axis=0.82 AU
Perihelion=0.49 AU
Aphelion=1.14 AU
Eccentricity=0.397
Inclination=5.81 deg
Longitude of ascending node=326.14 deg
Argument of perihelion=40.45 deg
Mean anomaly=120.04 deg
Orbital Period=271.16 days
Time of perihelion=2022-Nov-26
Mean diameter=46 meter
Absolute magnitude=24.3.

2023 DW - Valentine Asteroid trajectory

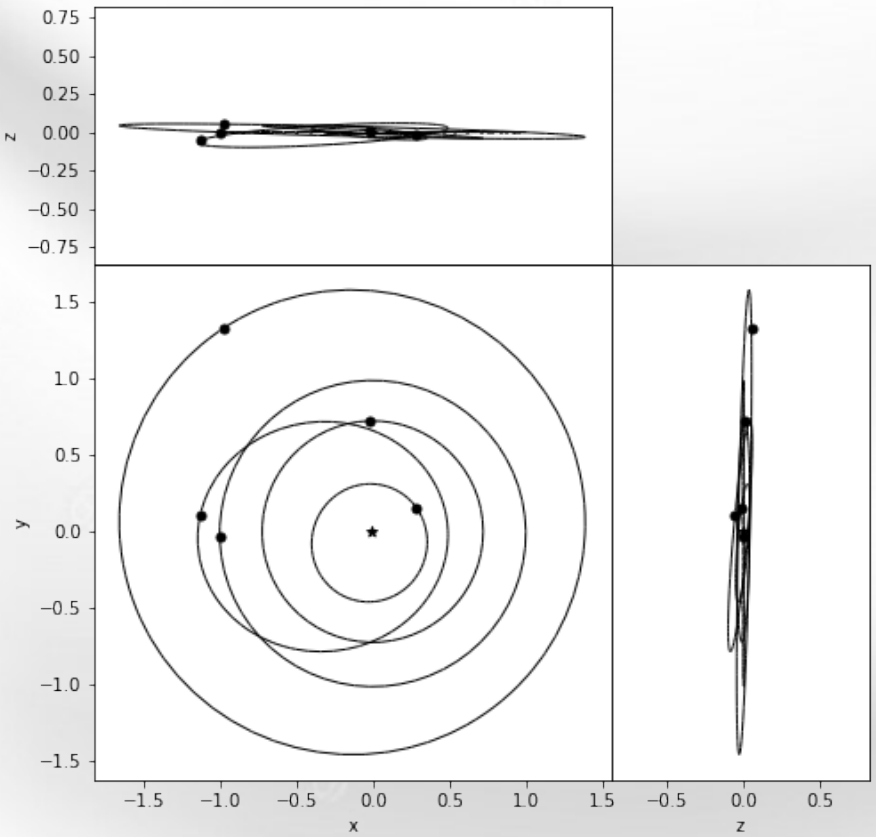

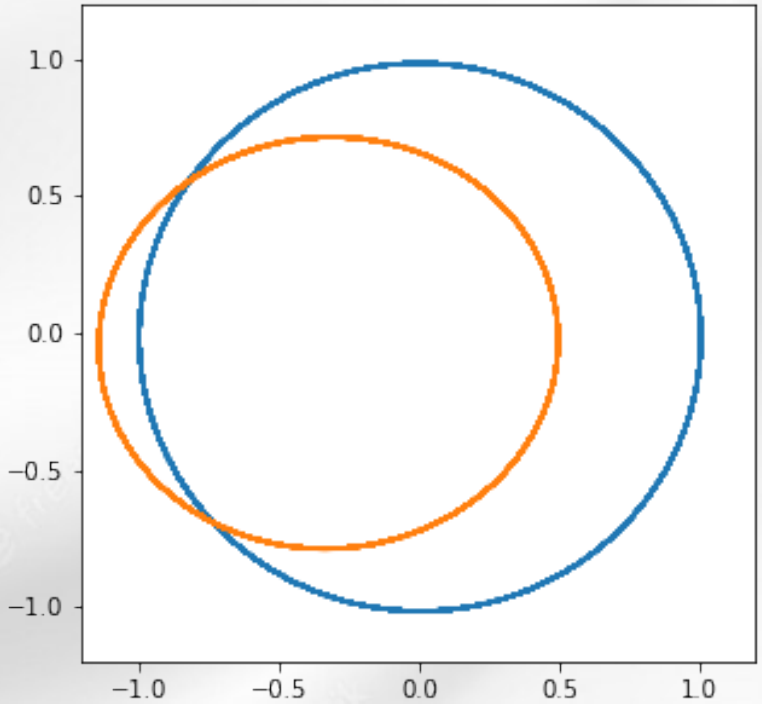

2023 DW - distance with Rebound

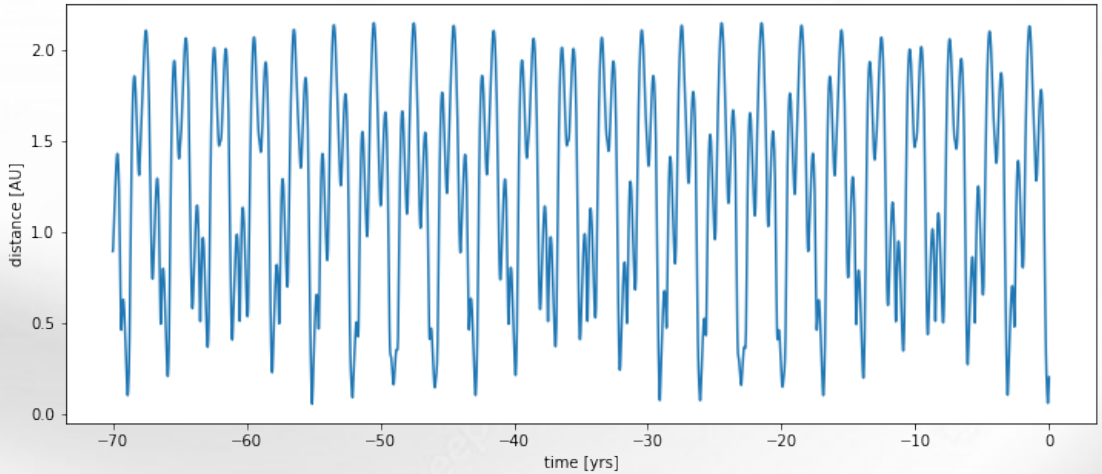

Minimum distance (0.053067 AU) occured at time: -55.102510 years: 1968-02-14

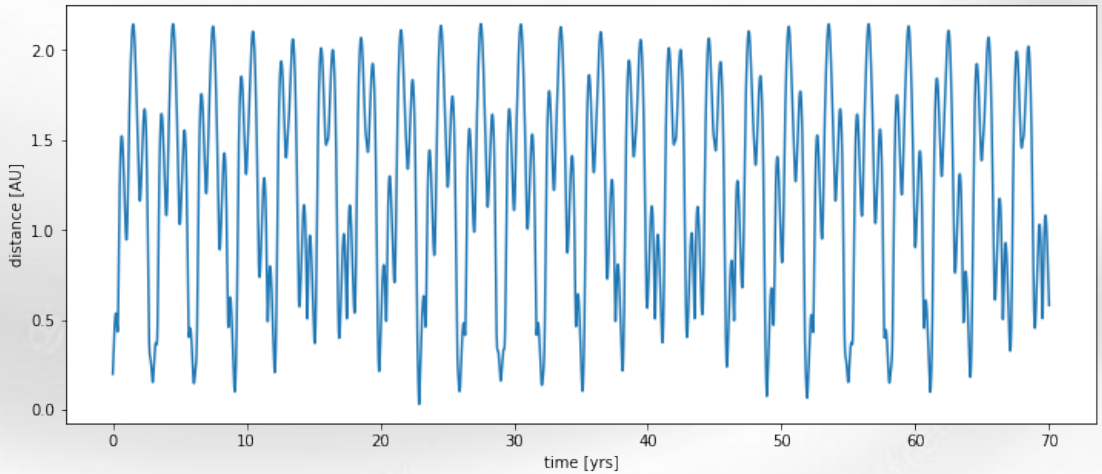

Minimum distance (0.032505 AU) occured at time: 22.899290 years: 2046-02-14

Earth-Moon distance = 0.002569 AU

2023 DW - Valentine Asteroid trajectory

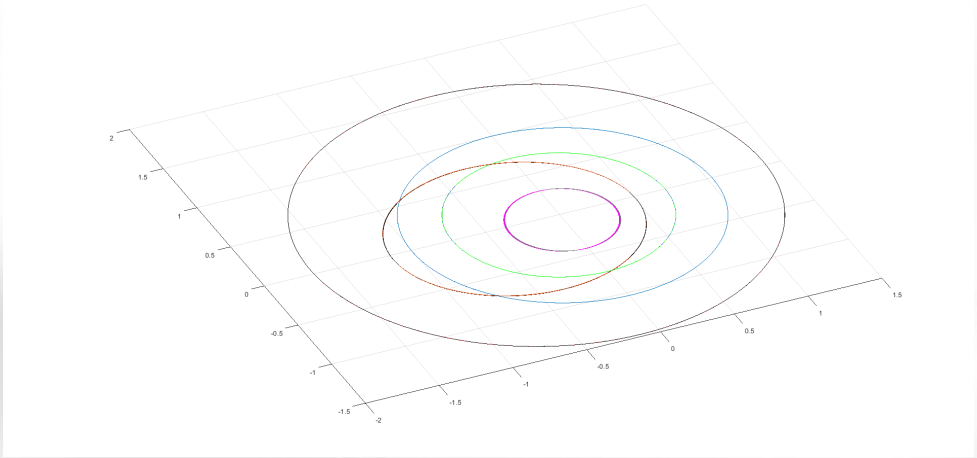

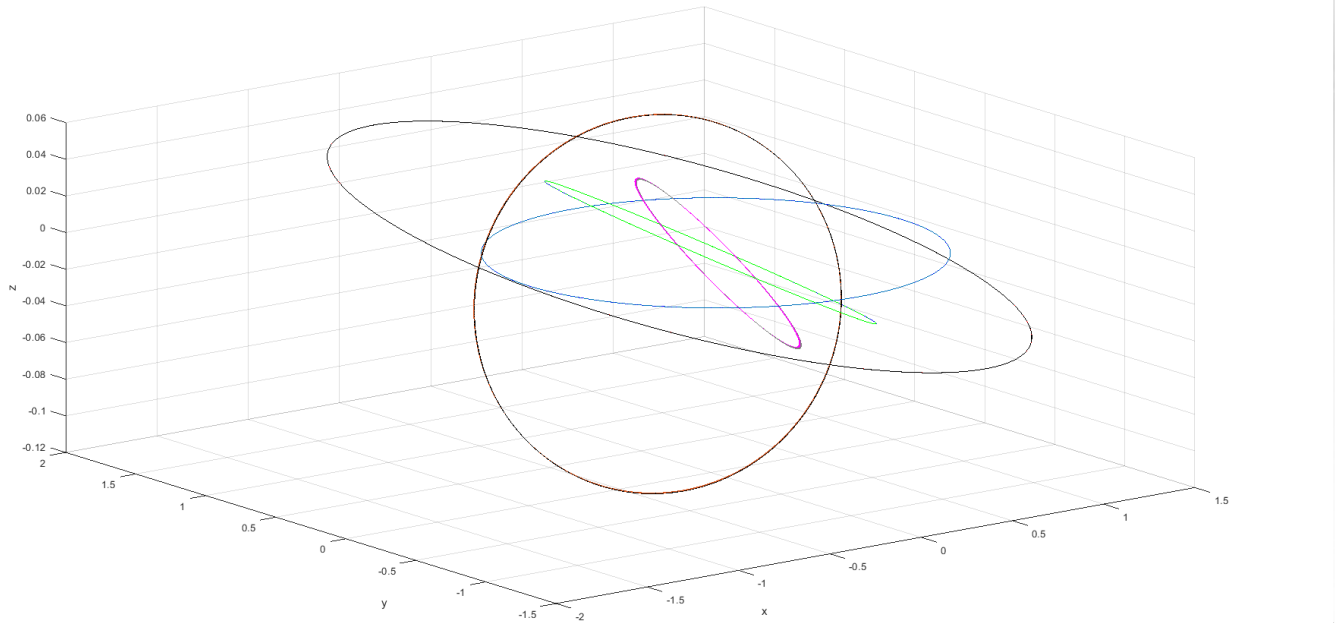

2023 DW - distance with Neri4

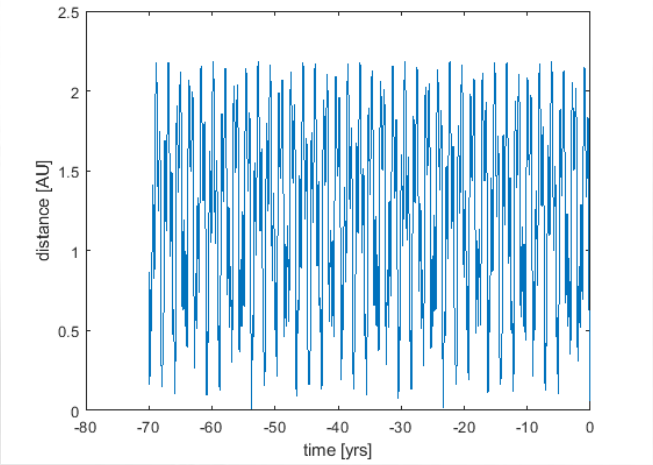

Minimum distance (0.01 AU) occured at time: -53.7274 years: 1970

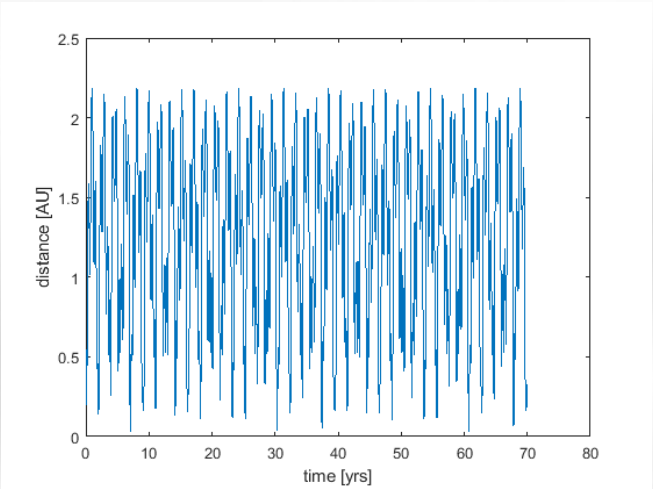

Minimum distance (0.0302 AU) occured at time: 60.7168 years: 2083

Earth-Moon distance = 0.002569 AU

News of the weekend - 2023 DZ2

2023 DZ2 is an asteroid roughly 70 meters in diameter, classified as a near-Earth object of the Apollo group, and originally a Virtual Impactor (VI). It was first observed on 27 February 2023, when it was 0.11 AU (16 million km) from Earth, with the Isaac Newton Telescope by Ovidiu Vaduvescu, Freya Barwell, and Kiran Jhass (ING and University of Sheffield student support astronomers) within the EURONEAR project.

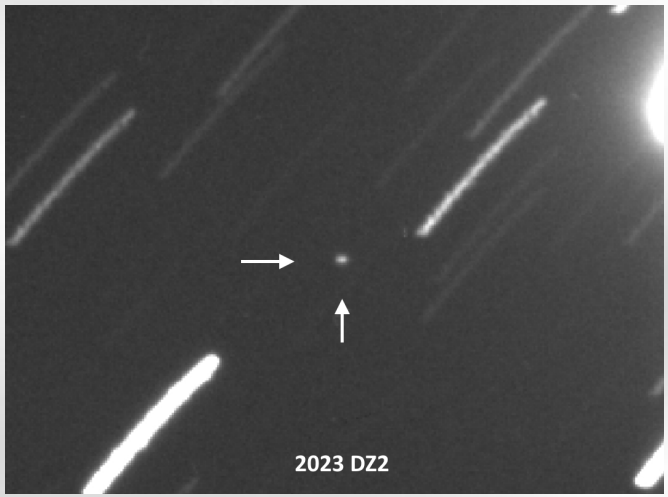

On 2023-03-21 I observed asteroid 2023 DZ2 remotely at 0.355-m telescope of Abbey Ridge Observatory (Canada)

2023 DZ2. Neo/Apollo (Orbital elements)

Discovered by Euronear at 27 February 2023.
Epoch 2023-Feb-25 (JD 2460000.5), Time of perihelion=2023-Apr-04
Mean diameter=70 meter, Absolute mag.=24.2, Apparent mag.=10.

Semi-major axis=2.15 AU
Perihelion=0.99 AU
Aphelion=3.31 AU
Eccentricity=0.53
Inclination=0.08 deg
Longitude of asc. node=187.91 deg
Argument of perihelion=5.96 deg
Mean anomaly= 348.67 deg
Orbital period = 3.16 years

Semi-major axis=2.08 AU
Perihelion=0.99 AU
Aphelion=3.16 AU
Eccentricity=0.52
Inclination=0.002 deg
Longitude of asc. node=-3.03 deg
Argument of perihelion=0.17 deg
Mean anomaly= 6.19 deg
Orbital period = 3 years

2023 DZ2 - trajectory (Rebound)

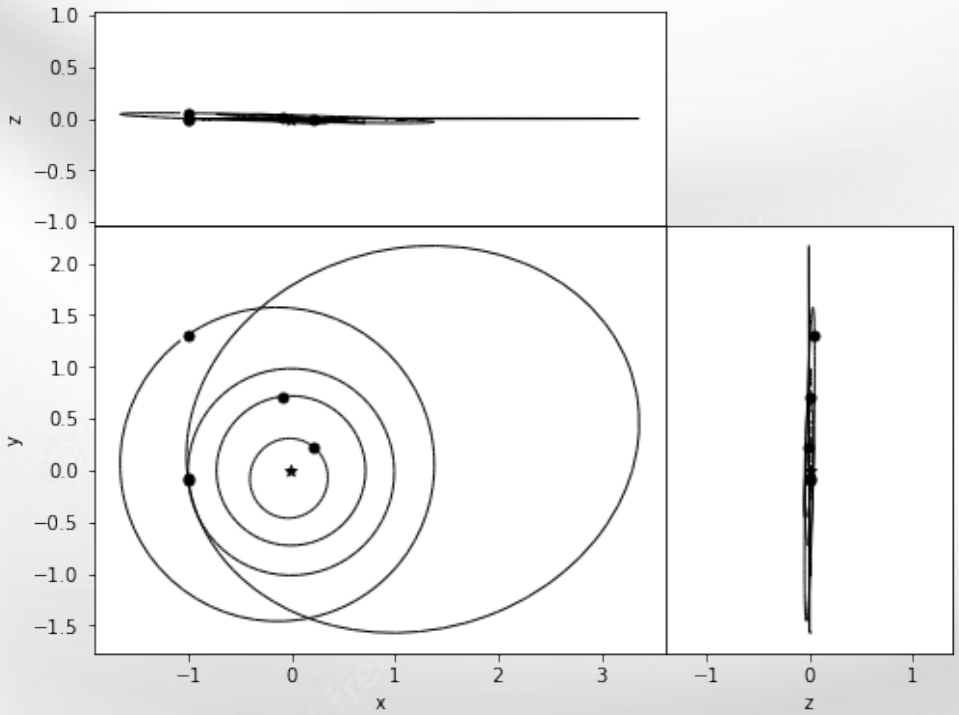

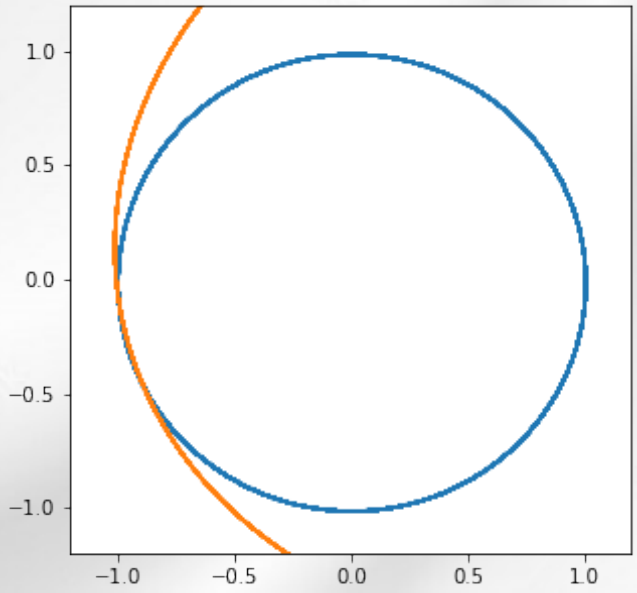

2023 DZ2 distance to Earth (Rebound)

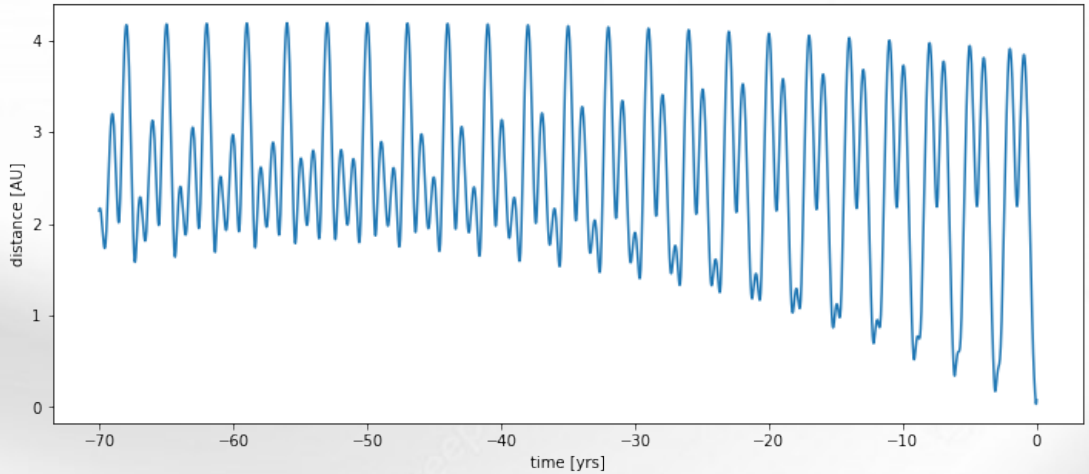

Minimum distance (0.03 AU) occured at time: -0.04 years: 2023-03-13

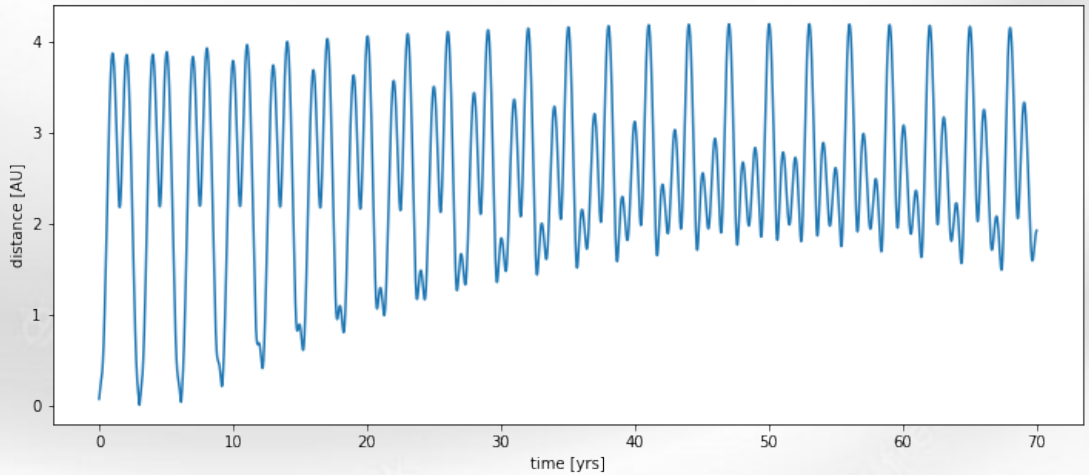

Minimum distance (0.008 AU) occured at time: 3.017302 years: 2026-04-03

2023 DZ2 - trajectory (Neri4)

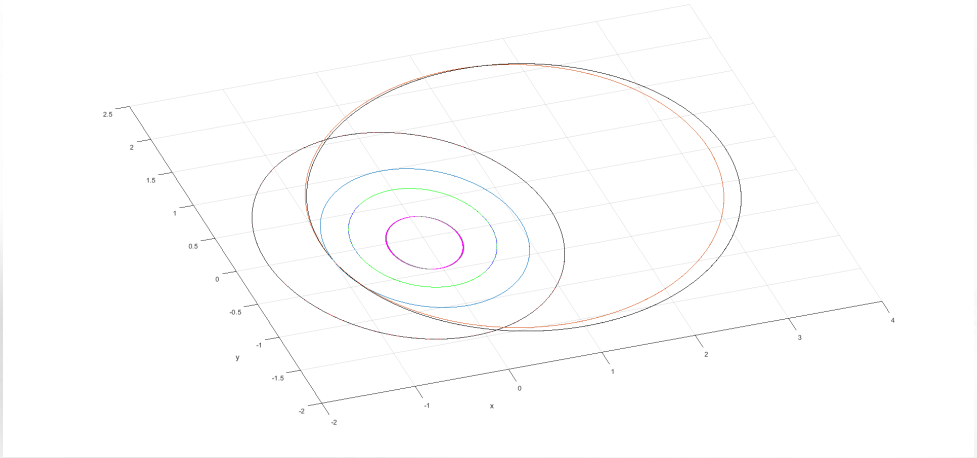

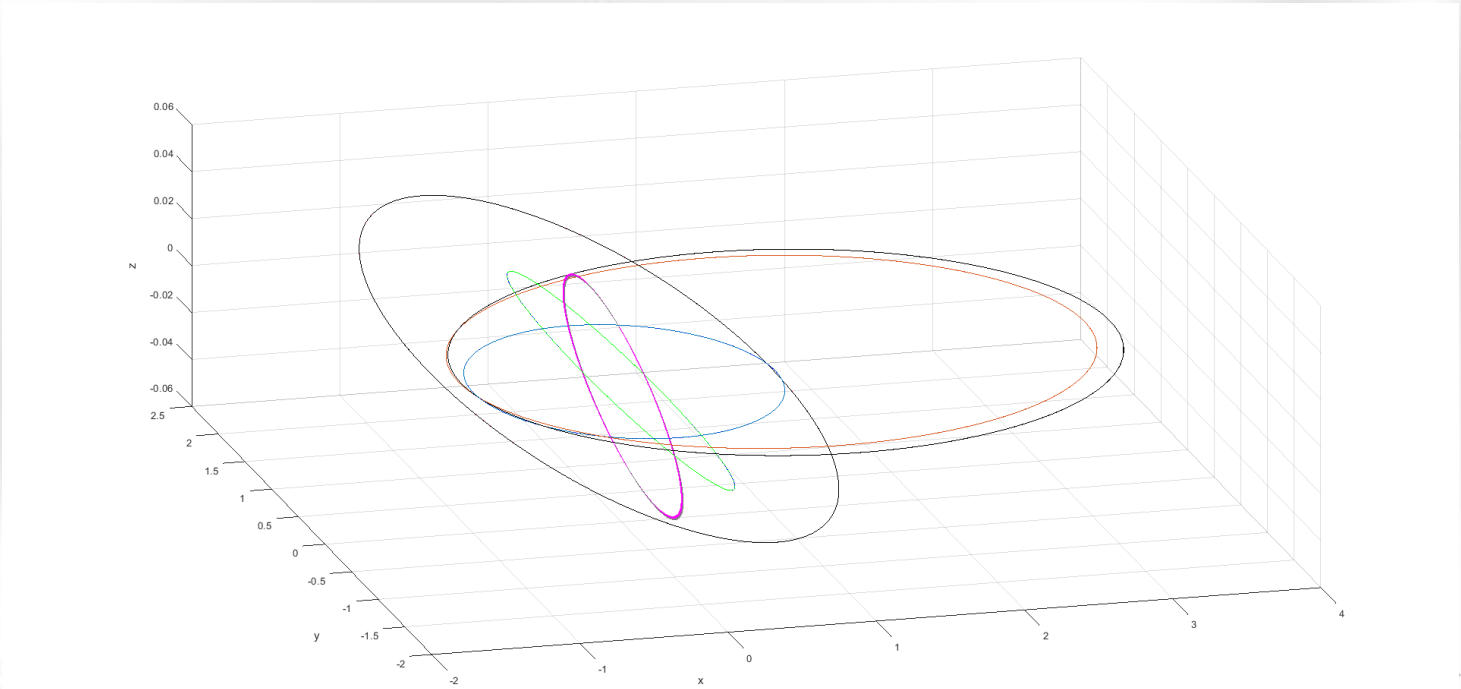

2023 DZ2 distance to Earth (Neri4)

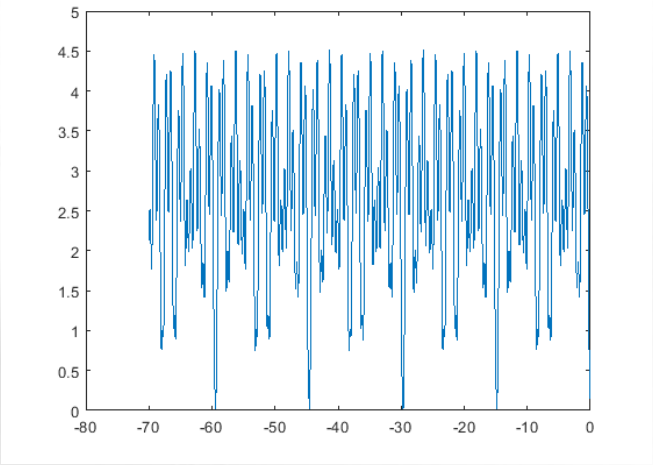

Minimum distance (0.002 AU) occured at time: -14.81 years: 2009

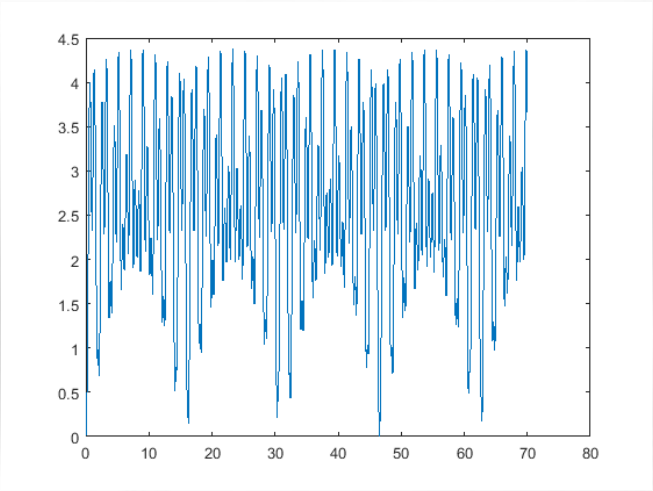

Minimum distance (0.008 AU) occured at time: 46.55 years: 2069

Close approach

From 1950 to 2150							
Planet	Date	MJD	Nominal distance (au)	Min. possible distance (au)	Stretching (au)	Width (au)	Close app. probability
EARTH	1951/05/16.41653	33782.4	0.1004130	0.0993730	5.159e-3	1.685e-7	1.00e+0
EARTH	1961/03/08.86976	37366.9	0.0676641	0.0343266	1.505e-2	2.743e-7	1.00e+0
6	1991/07/06.44616	48443.4	0.0102151	0.0092133	4.239e-3	9.003e-7	9.48e-1
EARTH	2004/04/18.99241	53114.0	0.0008731	0.0008670	3.047e-6	7.849e-9	1.00e+0
MARS	2020/04/30.07630	58969.1	0.0380028	0.0380001	1.105e-6	2.763e-8	1.00e+0
EARTH	2023/03/25.82678	60028.8	0.0011674	0.0011674	4.967e-10	4.445e-10	1.00e+0
EARTH	2026/04/04.08417	61134.1	0.0067667	0.0067664	2.057e-7	2.980e-9	1.00e+0
EARTH	2029/05/02.89573	62258.9	0.0248940	0.0248898	2.562e-6	1.067e-8	1.00e+0
EARTH	2032/05/25.12168	63377.1	0.1933820	0.1933770	2.123e-6	1.392e-8	1.00e+0

Lunar distance $= 0.002569$ AU

2023 DZ2 - Real Time Close Approach

2023 DZ2 Asteroid passed 174,638 $\pm$ 26 km (0.0011 AU) of Earth on March 25, 2023. This is a little less than half the distance to the Moon. This was the largest asteroid to approach this close since 2019 OK [25 July 2019 it had its closest approach to Earth, when it passed about 0.00047697 AU = 71,354 km—less than one-fifth of the distance to the Moon].
The discovery was carried out within the (Data-parallel detection of Solar System objects and space debris) ParaSOL project that is sponsored by UEFISCDI in Romania and led by Marcel Popescu. The new NEA was identified by Costin Boldea and by the STU ParaSOL software pipeline developed by the amateur astronomer Malin Stanescu. Other members of the EURONEAR collaboration who participated in the data analysis were Marian Predatu, and the amateur astronomers Lucian Curelaru and Daniel Bertesteanu.

Conclusion

- The purpose of the formalistic approach (Hamiltonian dynamics and canonical transformations) in dynamics is to furnish such formulations of dynamical problems as are best suited for analytical and numerical undertakings.
- Regularization methods are indicative of numerical effectiveness. The key to the further progress of numerical integrators lies in the improved treatment of close encounters that control the dynamical evolution.
- Comparing some software packages (i.e. REBOUND, STARLAB, etc.) that can integrate the motion of n particles under the influence of gravity using symplectic, hybrid symplectic, and non-symplectic integrators seems that simultaneous close encounters slow down the integrators.
- These integrators must be attentively adapted and well know their properties to avoid unrealistic results. High-performance computer and artificial intelligence should be the key to future research.

Thank you for your attention!

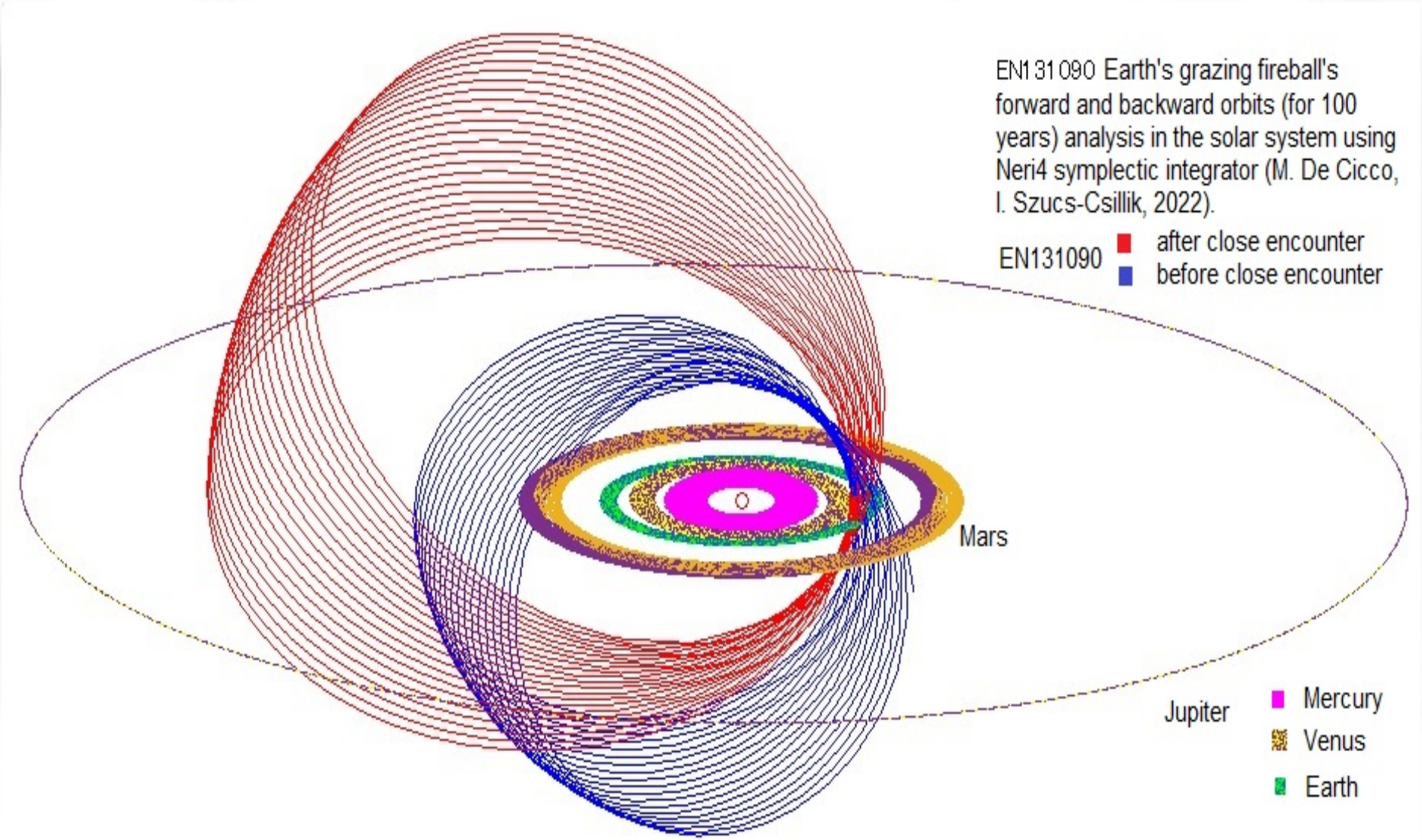

Elements of the EN131090 meteoroid before and after from Borovicka and Ceplecha (1992) updated for J2000.0

Heliocentric orbits parameters (J.2000.0)		
	before	after
α_G	$97^\circ.67 \pm 0^\circ.01$	$97^\circ.28 \pm 0^\circ.01$
δ_G	$-40^\circ.58 \pm 0^\circ.01$	$-36^\circ.34 \pm 0^\circ.01$
v_G	40.22 ± 0.17km/s	40.22 ± 0.17km/s
a	2.72 ± 0.08AU	1.87 ± 0.03 AU
P	4.5 ± 0.2yr	2.56 ± 0.06yr
e	0.64 ± 0.01	0.473 ± 0.009
q	0.9923 ± 0.0001 AU	0.9844 ± 0.0002 AU
Q	4.45 ± 0.15 AU	2.76 ± 0.07AU
ω	$9^\circ.60 \pm 0^\circ.01$	$16^\circ.60 \pm 0^\circ.02$
Ω	$18^\circ.973$	$19^\circ.672$
i	$71^\circ.39 \pm 0^\circ.02$	$74^\circ.40 \pm 0^\circ.02$

Considering the values of brightness that changed very few, which minimum is M:−5.96 and reach a maximum M: −6.45 during the perigee approach, velocity variations were so small that V: 41.74 ± 0.24 km/sec, can be estimated constant, so with air drag deceleration determined at perigee point, the authors concluded that far most probable fireball is an ordinary chondrite, with an initial mass of 44 kg and loss of 0.35 kg.